12

Beamforming Based on Finite-Rate Feedback

Pengcheng Zhu[1], Lan Tang[2], Yan Wang[3], Xiaohu You[4]
[1,3,4]*National Mobile Communications Research Laboratory*
Southeast University, Nanjing, 210096
[4]*School of Electrical Science and Engineering*
Nanjing University, Nanjing, 210093
P. R. China

1. Introduction

Multiple-input multi-output (MIMO), emerged as one of the most significant breakthroughs in wireless communications theory over the last two decades, is considered as a key to meeting the increasing demands for high data rates and mass wireless access services over a limited spectrum bandwidth. Transmit beamforming with receive combining is a low-complexity technique to exploit the benefits of MIMO wireless systems. It has received much interest over the last few years, because it provides substantial performance improvement without sophisticated signal processing. In order to enable the beamforming operation, either full or partial channel state information (CSI) has to be furnished to the transmitter. With full CSI, the optimal transmit beamforming scheme is maximum ratio transmission (MRT) [Dighe et al. (2003a)], where the principal right singular vector of the channel matrix is used as the beamforming vector. In Rayleigh fading, exact expressions for the symbol error rate (SER) of MRT were derived in [Dighe et al. (2003a;b)], and the asymptotic error performance was studied in [Zhou & Dai (2006)].

However, in certain application scenarios, e.g. frequency division duplex (FDD) systems, CSI is not usually available at the transmitter. To cope with the lack of CSI, a beamforming scheme based on finite-rate feedback has been proposed in the literature, where the CSI is quantized at the receiver and fed back to the transmitter. This scheme has been adopted in current 3GPP specifications. Under the assumption of independent block-fading and the assumption of delay- and error-free feedback, the design and performance analysis of quantized beamforming systems have been well investigated. Different beamformer design methods were developed in [Mukkavilli et al. (2003); Love & Heath (2003); Xia & Giannakis (2006)]. In multiple-input single-output (MISO) cases, lower bounds to the outage probability and symbol error rate (SER) were derived in [Mukkavilli et al. (2003)] and [Zhou et al. (2005)], respectively. In MIMO cases, the average receive signal-to-noise ratio (SNR) and outage probability were studied in [Mondal & Heath (2006)]. Analytical results showed that full diversity order can be achieved by a well-designed beamformer [Love & Heath (2005)].

This chapter highlights recent advances in beamforming based on finite-rate feedback from a communication-theoretic perspective. We first study the SER performance when the feedback link is delay- and error-free. Then non-ideal factors in the feedback link are investigated, and countermeasures are proposed to compensate the performance degradation due to non-ideal feedback.

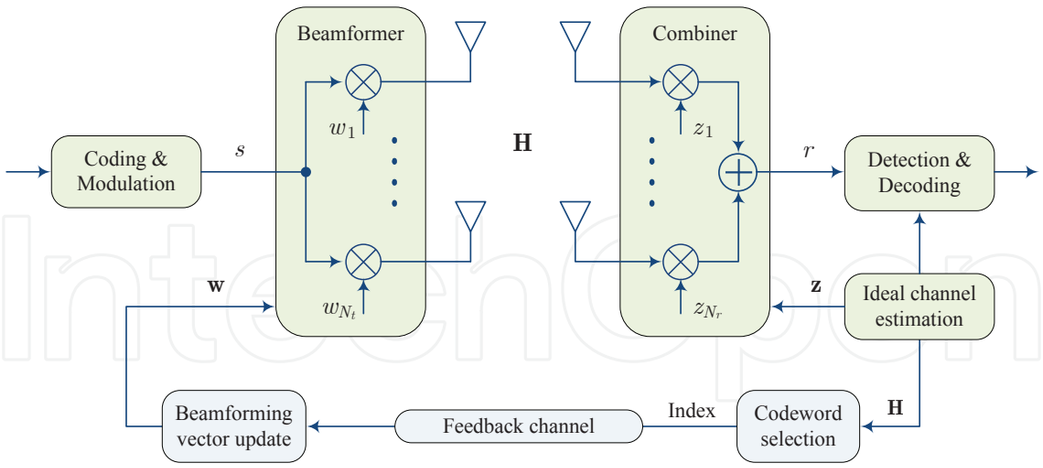

Fig. 1. A beamforming system based on finite-rate feedback.

The notations used in this chapter are conformed to the following convention. Bold upper and lower case letters are used to denote matrices and column vectors, respectively. $(\cdot)^T$, and $(\cdot)^*$ refer to transpose and conjugate transpose, respectively. $\|\cdot\|$ and $\|\cdot\|_{\mathrm{F}}$ stand for vector 2-norm and matrix Frobenius norm, respectively. $\mathbf{I}_N$ refers to the $N \times N$ identity matrix. $\mathcal{CN}(\mu, \sigma^2)$ stands for the circularly symmetric complex Gaussian distribution with mean μ and covariance σ^2. Pr and $\mathbb{E}$ denote the probability and expectation operators, respectively.

2. An upper bound on the SER

In this section, we evaluate the SER of a beamforming system based on finite-rate feedback. Assuming a delay- and error-free feedback link, we derive an upper bound on the average SER, and prove that the bound is asymptotically tight in high SNR regions.

2.1 System model

Consider an MIMO system with N_t transmit and N_r receive antennas. The wireless channel is assumed to be frequency-flat, and is modeled as an $N_r \times N_t$ random matrix $\mathbf{H}$. The (m, n)-th entry of the channel matrix, $h_{m,n}$, denotes the fading coefficient between the n-th transmit antenna and the m-th receive antenna. We assume an independent and identically distributed (i.i.d.) Rayleigh fading. Then the fading coefficient $h_{m,n}$'s are independent of each other and distributed as $\mathcal{CN}(0, 1)$.

The system adopts transmit beamforming with receive combining, as shown in Figure 1. At the transmitter, the information-bearing symbol $s \in \mathbb{C}$ is weighted by a beamforming vector, and transmitted simultaneously from all antennas. Then the $N_t \times 1$ transmitted signal vector is given by $\mathbf{x} = \mathbf{w}\, s$, where $\mathbf{w} = [w_1, \cdots, w_{N_t}]^T$ denotes the beamforming vector. The beamforming vector is a unit-norm vector, satisfying $\|\mathbf{w}\| = 1$. At the receiver, the $N_r \times 1$ received signal vector can be expressed as

$$\mathbf{y} = \mathbf{H}\mathbf{w}\, s + \boldsymbol{\eta}, \tag{1}$$

where $\boldsymbol{\eta}$ refers to the noise vector with independent $\mathcal{CN}(0, N_0)$ entries. Assuming that the receiver knows the channel $\mathbf{H}$ and the beamforming vector $\mathbf{w}$, it performs receive combining

to the received signal, using the maximum ratio combining (MRC) vector [Love & Heath (2003)]

$$\mathbf{z} = \frac{\mathbf{Hw}}{\|\mathbf{Hw}\|}.$$

The signal $r \in \mathbb{C}$ after receive combining can be written as

$$r = \mathbf{z}^*\mathbf{y} = \mathbf{z}^*\mathbf{Hw}\,s + \mathbf{z}^*\boldsymbol{\eta}, \tag{2}$$

and the corresponding instantaneous *receive SNR* is given by

$$\gamma = \gamma_S \|\mathbf{Hw}\|^2, \tag{3}$$

where

$$\gamma_S \triangleq \mathbb{E}(|s|^2)/N_0 \tag{4}$$

is the average *symbol SNR*.

In a beamforming system based on finite-rate feedback, the beamforming vector $\mathbf{w}$ is restricted to lie in a finite set (codebook) that is known to both the transmitter and receiver. The codebook, denoted as $\mathcal{C}$, is designed in advance and consists of $N_c = 2^B$ unit-norm codewords $\mathcal{C} = \{\mathbf{c}_1, \cdots, \mathbf{c}_{N_c}\}$. The receiver selects the favorable codeword from the codebook according to

$$\mathbf{c}_{\text{opt}} = \arg\max_{\mathbf{c}\in\mathcal{C}} \|\mathbf{Hc}\|^2. \tag{5}$$

If the codeword $\mathbf{c}_k$ is selected ($\mathbf{c}_{\text{opt}} = \mathbf{c}_k$), its index k is sent to the transmitter via a feedback link, requiring B bits each time. In this section, we focus on the case of delay- and error-free feedback. The transmitter obtains the index of the optimal codeword, and uses the codeword as beamforming vector. Then we have

$$\mathbf{w} = \mathbf{c}_{\text{opt}} \quad \text{(delay- and error-free feedback)}. \tag{6}$$

As in [Love & Heath (2005)], we assume the beamforming codewords $\{\mathbf{c}_1, \cdots, \mathbf{c}_{N_c}\}$ span $\mathbb{C}^{N_t}$. This property guarantees the soundness of several steps in the following derivation. We note that it is a mild condition. To our knowledge, all well-designed codebooks, e.g. those in [Love & Heath (2003); Xia & Giannakis (2006)] and 3GPP specifications, satisfy this condition.

2.2 SER analysis

For notation brevity, phase-shift keying (PSK) signals are assumed in the derivations. Conditioned on the instantaneous SNR γ, the SER of M-ary PSK can be expressed as [Simon & Alouini (2005), Eq.(8.23)]

$$P_E = \frac{1}{\pi}\int_0^{\frac{(M-1)\pi}{M}} \exp\left(-\frac{g_{\text{PSK}}\gamma}{\sin^2\theta}\right) \mathrm{d}\theta, \tag{7}$$

where $g_{\text{PSK}} = \sin^2(\pi/M)$ is a constellation-dependent constant. Applying (6) and (5) to (3), the instantaneous SNR of the beamforming system is given by

$$\gamma = \gamma_S\|\mathbf{Hw}\|^2 = \gamma_S\|\mathbf{Hc}_{\text{opt}}\|^2 = \gamma_S \max_{\mathbf{c}\in\mathcal{C}} \|\mathbf{Hc}\|^2 \tag{8}$$

Then substituting (8) into (7) and taking expectation, the average SER of the beamforming system can be written as

$$\overline{P}_E \triangleq \mathbb{E}\,P_E = \frac{1}{\pi}\int_0^{\frac{(M-1)\pi}{M}} \mathbb{E}\exp\left(-\frac{g_{\text{PSK}}\gamma_S}{\sin^2\theta}\max_{\mathbf{c}\in\mathcal{C}}\|\mathbf{Hc}\|^2\right) \mathrm{d}\theta, \tag{9}$$

where the expectation is respect to the channel matrix $\mathbf{H}$.
To find an upper bound on the average SER, we first study the expectation term in the right-hand-side of (9), as shown in the following lemma.

Lemma 1. *Let* $\mathbf{H}$ *be an* $N_r \times N_t$ *random matrix with i.i.d.* $\mathcal{CN}(0,1)$ *entries, and define*

$$\tilde{\mathbf{H}} \triangleq \mathbf{H}/\|\mathbf{H}\|_{\mathrm{F}}\,.$$

Then for a given beamforming codebook $\mathcal{C}$*, and a given* $t \geq 0$*, we have*

$$\mathbb{E}\,\exp\Big(-t\cdot\max_{\mathbf{c}\in\mathcal{C}}\|\mathbf{H}\mathbf{c}\|^2\Big) \leq \big(1+t\cdot g_{\mathrm{CB}}\big)^{-N_tN_r}, \tag{10}$$

where

$$g_{\mathrm{CB}} \triangleq \Big[\mathbb{E}\Big\{\big(\max_{\mathbf{c}\in\mathcal{C}}\|\tilde{\mathbf{H}}\mathbf{c}\|^2\big)^{-N_tN_r}\Big\}\Big]^{-\frac{1}{N_tN_r}} \tag{11}$$

is a codebook-dependent parameter.
Proof: Since the channel matrix $\mathbf{H}$ has i.i.d. $\mathcal{CN}(0,1)$ entries, $\|\mathbf{H}\|_{\mathrm{F}}^2$ is chi-square distributed and independent of $\tilde{\mathbf{H}}$. The moment generating function of $\|\mathbf{H}\|_{\mathrm{F}}^2$ is given by

$$\mathbb{E}\,\exp\Big(-s\|\mathbf{H}\|_{\mathrm{F}}^2\Big) = (1+s)^{-N_tN_r}. \tag{12}$$

Therefore we have

$$\begin{aligned}\mathbb{E}\,\exp\big(-t\cdot\max_{\mathbf{c}\in\mathcal{C}}\|\mathbf{H}\mathbf{c}\|^2\big) &= \mathbb{E}\Big\{\mathbb{E}\Big[\exp\Big(-t\cdot\|\mathbf{H}\|_{\mathrm{F}}^2\cdot\max_{\mathbf{c}\in\mathcal{C}}\|\tilde{\mathbf{H}}\mathbf{c}\|^2\Big)\Big|\tilde{\mathbf{H}}\Big]\Big\}\\ &= \mathbb{E}\Big\{\big(1+t\cdot\max_{\mathbf{c}\in\mathcal{C}}\|\tilde{\mathbf{H}}\mathbf{c}\|^2\big)^{-N_tN_r}\Big\}.\end{aligned} \tag{13}$$

Notice that when $x, t > 0$,

$$f(x) = \Big(1+t\cdot x^{-\frac{1}{N_tN_r}}\Big)^{-N_tN_r}$$

is a concave function with respect to x. We can apply Jensen's inequality to the right-hand-side of (13), and obtain

$$\begin{aligned}\mathbb{E}\Big\{\big(1+t\cdot\max_{\mathbf{c}\in\mathcal{C}}\|\tilde{\mathbf{H}}\mathbf{c}\|^2\big)^{-N_tN_r}\Big\} &= \mathbb{E}\Bigg\{\Bigg(1+t\cdot\Big[\underbrace{\big(\max_{\mathbf{c}\in\mathcal{C}}\|\tilde{\mathbf{H}}\mathbf{c}\|^2\big)^{-N_tN_r}}_{\text{treated as a r. v.}}\Big]^{-\frac{1}{N_tN_r}}\Bigg)^{-N_tN_r}\Bigg\}\\ &\leq \Bigg(1+t\cdot\Big[\mathbb{E}\Big\{\big(\max_{\mathbf{c}\in\mathcal{C}}\|\tilde{\mathbf{H}}\mathbf{c}\|^2\big)^{-N_tN_r}\Big\}\Big]^{-\frac{1}{N_tN_r}}\Bigg)^{-N_tN_r}.\end{aligned} \tag{14}$$

Substituting this into (13), we reach the desired result (10). □

In Lemma 1, the definition of g_{CB} is not given in a closed-form. Its value has to be evaluated numerically. In the following lemma, we will further study the parameter, and derive a closed-form approximation for it.

Lemma 2. *The parameter* g_{CB} *satisfies* $0 \leq g_{\mathrm{CB}} \leq 1$*. Moreover, for a well-designed codebook, it can be approximated by*

$$g_{\mathrm{CB}}^{-N_tN_r} \simeq N_cC_1(N_tN_r-1)!\,(N_t-1)\sum_{n=0}^{N_t-2}\binom{N_t-2}{n}\frac{(-1)^n(C_2^{-(N_tN_r-1-n)}-1)}{N_tN_r-1-n}, \tag{15}$$

where

$$C_1 \triangleq N_t N_r \prod_{n=1}^{\min(N_t,N_r)} \frac{[\min(N_t,N_r)-n]!}{(N_t+N_r-n)!} \tag{16}$$

and

$$C_2 \triangleq 1-\left(1/N_c\right)^{\frac{1}{N_t-1}}. \tag{17}$$

Proof: We first prove $0 \le g_{\mathrm{CB}} \le 1$. It is clear from the definition that $g_{\mathrm{CB}} \ge 0$. To see $g_{\mathrm{CB}} \le 1$, consider the following equality

$$\begin{aligned}\lim_{t\to\infty} t^{N_tN_r}\mathbb{E}\Big\{\big(1+t\cdot\max_{\mathbf{c}\in\mathcal{C}}\|\tilde{\mathbf{H}}\mathbf{c}\|^2\big)^{-N_tN_r}\Big\} &= \mathbb{E}\Big\{\lim_{t\to\infty} t^{N_tN_r}\big(1+t\cdot\max_{\mathbf{c}\in\mathcal{C}}\|\tilde{\mathbf{H}}\mathbf{c}\|^2\big)^{-N_tN_r}\Big\}\\ &= \mathbb{E}\Big\{\big(\max_{\mathbf{c}\in\mathcal{C}}\|\tilde{\mathbf{H}}\mathbf{c}\|^2\big)^{-N_tN_r}\Big\}. \end{aligned}\tag{18}$$

By the definition (11), (18) implies that

$$g_{\mathrm{CB}}^{-N_tN_r} = \lim_{t\to\infty} t^{N_tN_r}\mathbb{E}\Big\{\big(1+t\cdot\max_{\mathbf{c}\in\mathcal{C}}\|\tilde{\mathbf{H}}\mathbf{c}\|^2\big)^{-N_tN_r}\Big\} \tag{19}$$

Notice that $\|\tilde{\mathbf{H}}\|_{\mathrm{F}}=1$ and $\|\mathbf{c}\|=1, \forall \mathbf{c}\in\mathcal{C}$. Therefore

$$\max_{\mathbf{c}\in\mathcal{C}}\|\tilde{\mathbf{H}}\mathbf{c}\|^2 \le 1$$

and

$$\mathbb{E}\Big\{\big(1+t\cdot\max_{\mathbf{c}\in\mathcal{C}}\|\tilde{\mathbf{H}}\mathbf{c}\|^2\big)^{-N_tN_r}\Big\} \ge (1+t)^{-N_tN_r}.$$

So we have

$$\begin{aligned} g_{\mathrm{CB}}^{-N_tN_r} &= \lim_{t\to\infty} t^{N_tN_r}\mathbb{E}\Big\{\big(1+t\cdot\max_{\mathbf{c}\in\mathcal{C}}\|\tilde{\mathbf{H}}\mathbf{c}\|^2\big)^{-N_tN_r}\Big\}\\ &\ge \lim_{t\to\infty} t^{N_tN_r}(1+t)^{-N_tN_r}\\ &= 1\,, \end{aligned}\tag{20}$$

which implies $\beta_{\mathcal{C}} \le 1$.
To obtain (15), recall Equation (13) in the proof of Lemma 1. Substituting it into (19) yields

$$g_{\mathrm{CB}}^{-N_tN_r} = \lim_{t\to\infty} t^{N_tN_r}\,\mathbb{E}\,\exp\big(-t\cdot\max_{\mathbf{c}\in\mathcal{C}}\|\mathbf{H}\mathbf{c}\|^2\big). \tag{21}$$

Let the eigen-decomposition of the channel be denoted as

$$\mathbf{H}^*\mathbf{H} = \begin{bmatrix}\mathbf{u}_1,\cdots,\mathbf{u}_{N_t}\end{bmatrix}\begin{bmatrix}\lambda_1 & & \\ & \ddots & \\ & & \lambda_{N_t}\end{bmatrix}\begin{bmatrix}\mathbf{u}_1^*\\ \vdots\\ \mathbf{u}_{N_t}^*\end{bmatrix} \tag{22}$$

where $\lambda_1 \ge \cdots \ge \lambda_{N_t} \ge 0$ and $\mathbf{u}_1,\cdots,\mathbf{u}_{N_t}$ denote the eigenvalues and the eigenvectors, respectively. We have the following inequality

$$\|\mathbf{H}\mathbf{c}\|^2 = \mathbf{c}^*\mathbf{H}^*\mathbf{H}\mathbf{c} = \sum_{n=1}^{N_t}\lambda_n|\mathbf{u}_n^*\mathbf{c}|^2 \ge \lambda_1|\mathbf{u}_1^*\mathbf{c}|^2. \tag{23}$$

Substituting (23) into (21), one obtains

$$g_{\mathrm{CB}}^{-N_tN_r} \le \lim_{t\to\infty} t^{N_tN_r}\,\mathbb{E}\,\exp\Big(-t\lambda_1\cdot\max_{\mathbf{c}\in\mathcal{C}}|\mathbf{u}_1^*\mathbf{c}|^2\Big). \tag{24}$$

In an i.i.d. Rayleigh fading scenario, $\mathbf{H}^*\mathbf{H}$ is Wishart distributed. The eigenvalue and eigenvector of a Wishart matrix are independent of each other. So (24) can be expressed as

$$\begin{aligned} g_{\mathrm{CB}}^{-N_tN_r} &\le \lim_{t\to\infty} t^{N_tN_r}\int\Big[\int_0^\infty e^{-txz}p_{\lambda_1}(x)\,\mathrm{d}x\Big]\mathrm{d}\Big(\Pr\Big\{\max_{\mathbf{c}\in\mathcal{C}}|\mathbf{u}_1^*\mathbf{c}|^2<z\Big\}\Big)\\ &= \int\Big[\lim_{t\to\infty} t^{N_tN_r}\int_0^\infty e^{-txz}p_{\lambda_1}(x)\,\mathrm{d}x\Big]\mathrm{d}\Big(\Pr\Big\{\max_{\mathbf{c}\in\mathcal{C}}|\mathbf{u}_1^*\mathbf{c}|^2<z\Big\}\Big) \end{aligned} \tag{25}$$

Since $\mathbf{H}^*\mathbf{H}$ is Wishart distributed, the probability density function (PDF) of its largest eigenvalue λ_1 has the asymptotic property [Zhou & Dai (2006)]

$$p_{\lambda_1}(x) = C_1\,x^{N_tN_r-1} + o(x^{N_tN_r-1}),\quad x\to 0^+, \tag{26}$$

where C_1 is defined in (16), and $o(x^{N_tN_r-1})$ stands for a function $a(x)$ satisfying $\lim_{x\to 0^+} a(x)/x^{N_tN_r-1}=0$. Then we have

$$\begin{aligned} \lim_{t\to\infty} t^{N_tN_r}\int_0^\infty e^{-txz}p_{\lambda_1}(x)\,\mathrm{d}x &= \lim_{t\to\infty} t^{N_tN_r}\int_0^\infty e^{-yz}p_{\lambda_1}(y/t)\,\mathrm{d}(y/t)\\ &= \int_0^\infty e^{-yz}\Big[\lim_{t\to\infty} t^{N_tN_r-1}p_{\lambda_1}(y/t)\Big]\mathrm{d}y\\ &= \int_0^\infty e^{-yz}C_1 y^{N_tN_r-1}\mathrm{d}y\\ &= C_1(N_tN_r-1)!\,z^{-N_tN_r} \end{aligned} \tag{27}$$

Substituting (27) into (25) yields

$$g_{\mathrm{CB}}^{-N_tN_r} \le C_1(N_tN_r-1)!\int z^{-N_tN_r}\mathrm{d}\Big(\Pr\Big\{\max_{\mathbf{c}\in\mathcal{C}}|\mathbf{u}_1^*\mathbf{c}|^2<z\Big\}\Big). \tag{28}$$

For a well-designed codebook, the Voronoi cells of the codewords can be approximated by 'spherical caps', which leads to a very tight bound [Zhou et al. (2005)]

$$\Pr\Big\{\max_{\mathbf{c}\in\mathcal{C}}|\mathbf{u}_1^*\mathbf{c}|^2<z\Big\} \ge 1-N_c(1-z)^{N_t-1},\quad C_2\le z\le 1, \tag{29}$$

where C_2 is defined in (17). The inequalities (28) and (29) are both tight. We now treat then as approximations, and substitute (29) into (28). After performing the integration, the right-hand-side of (15) is obtained. □

We then apply the results in Lemma 1 and 2 to the SER analysis. Setting $t = g_{\mathrm{PSK}}\gamma_S/\sin^2\theta$ and after some manipulations, (10) becomes

$$\mathbb{E}\,\exp\Big(-\frac{g_{\mathrm{PSK}}\gamma_S}{\sin^2\theta}\max_{\mathbf{c}\in\mathcal{C}}\|\mathbf{H}\mathbf{c}\|^2\Big) \le \left(\frac{\sin^2\theta}{g_{\mathrm{PSK}}g_{\mathrm{CB}}\gamma_S+\sin^2\theta}\right)^{N_tN_r}. \tag{30}$$

Substituting this into (9), we obtain an upper bound on the average SER of M-ary PSK signal

$$\overline{P}_E \le \overline{P}_E^{\mathrm{ub}} = \frac{1}{\pi}\int_0^{\frac{(M-1)\pi}{M}}\left(\frac{\sin^2\theta}{g_{\mathrm{PSK}}g_{\mathrm{CB}}\gamma_S+\sin^2\theta}\right)^{N_tN_r}\mathrm{d}\theta, \tag{31}$$

which is the main result of this section.

At last, we give two remarks on the SER bound.

Remark 1 (Asymptotic behavior). The upper bound has the merit of being asymptotically tight. In fact, at high SNR, we have

$$\begin{aligned} G &= \lim_{\gamma_S\to\infty} \gamma_S^{N_tN_r}\overline{P}_E \\ &\overset{(9)}{=} \frac{1}{\pi}\lim_{\gamma_S\to\infty} \gamma_S^{N_tN_r}\int_0^{\frac{(M-1)\pi}{M}} \mathbb{E}\exp\Big(-\frac{g_{\mathrm{PSK}}\gamma_S}{\sin^2\theta}\max_{\mathbf{c}\in\mathcal{C}}\|\mathbf{Hc}\|^2\Big)\,\mathrm{d}\theta \\ &= \frac{1}{\pi}\int_0^{\frac{(M-1)\pi}{M}} \left(\frac{\sin^2\theta}{g_{\mathrm{PSK}}}\right)^{N_tN_r}\left[\lim_{\gamma_S\to\infty}\left(\frac{g_{\mathrm{PSK}}\gamma_S}{\sin^2\theta}\right)^{N_tN_r}\mathbb{E}\exp\Big(-\frac{g_{\mathrm{PSK}}\gamma_S}{\sin^2\theta}\max_{\mathbf{c}\in\mathcal{C}}\|\mathbf{Hc}\|^2\Big)\right]\mathrm{d}\theta \\ &\overset{(21)}{=} \frac{1}{\pi}\int_0^{\frac{(M-1)\pi}{M}} \left(\frac{g_{\mathrm{PSK}}\gamma_S}{\sin^2\theta}\right)^{N_tN_r}(g_{\mathrm{CB}})^{-N_tN_r}\mathrm{d}\theta \\ &= \frac{1}{\pi}\int_0^{\frac{(M-1)\pi}{M}} \frac{(\sin\theta)^{2N_tN_r}}{(g_{\mathrm{PSK}}g_{\mathrm{CB}})^{N_tN_r}}\mathrm{d}\theta\,. \end{aligned} \tag{32}$$

This equation shows that as $\gamma_S\to\infty$, $\overline{P}_E$ decreases as $G\gamma_S^{-N_tN_r}+o(\gamma_S^{-N_tN_r})$. $G^{\frac{-1}{N_tN_r}}$ is usually referred to as the *coding gain*. On the other hand, it is easily verified that

$$\lim_{\gamma_S\to\infty}\gamma_S^{N_tN_r}\overline{P}_E^{\mathrm{ub}} = G\,.$$

Therefore, (31) is asymptotically tight at high SNR. Moreover, when $\gamma_S=0$, both sides of (31) are equal to $(M-1)/M$. So the bound holds with equality. This guarantees the tightness of the bound at low SNR.

Remark 2 (Extension to other constellations). For brevity, we have assumed a phase-shift keying (PSK) signal in the derivation of the SER bound. However, the same procedure can be applied to other 2-D constellations. For example, the SER of square quadrature amplitude modulation (QAM), conditioned on the instantaneous SNR γ, can be expressed as [Simon & Alouini (2005)]

$$P_{E,\mathrm{QAM}} = \frac{4(\sqrt{M}-1)}{\pi M}\int_0^{\pi/4}\exp\Big(-\frac{g_{\mathrm{QAM}}\gamma}{\sin^2\theta}\Big)\,\mathrm{d}\theta + \frac{4(\sqrt{M}-1)}{\pi\sqrt{M}}\int_{\pi/4}^{\pi/2}\exp\Big(-\frac{g_{\mathrm{QAM}}\gamma}{\sin^2\theta}\Big)\,\mathrm{d}\theta,$$

where M is the constellation size, and $g_{\mathrm{QAM}}=1.5/(M-1)$. This equation has a similar form to (7). Using the procedure of deriving (31), we can obtain an upper bound on the average SER of QAM

$$\begin{aligned} \overline{P}_{E,\mathrm{QAM}} = \mathbb{E}P_{E,\mathrm{QAM}} \le{}& \frac{4(\sqrt{M}-1)}{\pi M}\int_0^{\pi/4}\left(\frac{\sin^2\theta}{g_{\mathrm{QAM}}g_{\mathrm{CB}}\gamma_S+\sin^2\theta}\right)^{N_tN_r}\mathrm{d}\theta \\ &+\frac{4(\sqrt{M}-1)}{\pi\sqrt{M}}\int_{\pi/4}^{\pi/2}\left(\frac{\sin^2\theta}{g_{\mathrm{QAM}}g_{\mathrm{CB}}\gamma_S+\sin^2\theta}\right)^{N_tN_r}\mathrm{d}\theta\,. \end{aligned} \tag{33}$$

2.3 Extension to correlated rayleigh fading

In a correlated Rayleigh fading channel, the system model is the same as in Section 2.1, except that the channel matrix is modeled as

$$\mathrm{vec}(\mathbf{H}) = \mathbf{\Phi}\mathbf{h}_w, \tag{34}$$

where $\mathbf{h}_w$ refers to an $N_tN_r \times 1$ random vector with independent $\mathcal{CN}(0,1)$ entries; $\mathbf{\Phi}$ is an $N_tN_r \times N_tN_r$ positive definite matrix; and $\mathrm{vec}(\mathbf{H})$ denotes the $N_tN_r \times 1$ vector of stacked columns of $\mathbf{H}$. $\mathbf{\Phi}^2$ $(= \mathbf{\Phi}\mathbf{\Phi}^*)$ is usually called the channel correlation matrix.

The idea used in Section 2.2 can be extended to correlated Rayleigh fading scenarios. For M-ary PSK signals, we can prove that the average SER is upper bounded by

$$\overline{P}_E \leq \frac{1}{\pi}\int_0^{\frac{(M-1)\pi}{M}} \left(\frac{\sin^2\theta}{g_{\mathrm{PSK}}g_{\mathrm{CB}}g_{\mathrm{Cor}}\gamma_S + \sin^2\theta}\right)^{N_tN_r} \mathrm{d}\theta, \tag{35}$$

where

$$g_{\mathrm{Cor}} \triangleq \left[\det(\mathbf{\Phi}^2)\right]^{\frac{1}{N_tN_r}}$$

is a parameter depends on the channel correlation matrix. The proof of this bound is out of the scope of this book. Interesting readers are referred to [Zhu et al. (2010)] for detailed derivations.

The bound (35) is asymptotically tight at high and low SNRs [Zhu et al. (2010)]. However, at medium SNR, the tightness of the bound is not guaranteed because it does not fully reflect the effect of channel correlation. Based on extensive simulations, we propose the following conjectured SER formula

$$\overline{P}_E \overset{\text{conjectured}}{\leq} \frac{1}{\pi}\int_0^{\frac{(M-1)\pi}{M}} \prod_{i=1}^{N_tN_r} \frac{\sin^2\theta}{g_{\mathrm{PSK}}g_{\mathrm{CB}}\gamma_{\mathrm{S}}\lambda_{\mathbf{\Phi}^2,i} + \sin^2\theta}\,\mathrm{d}\theta, \tag{36}$$

where $\lambda_{\mathbf{\Phi}^2,i}$ denotes the i-th eigenvalue of $\mathbf{\Phi}^2$. We have not been able to prove the conjecture as yet. Some discussion in support of it is presented in [Zhu et al. (2010)].

2.4 Numerical results

Simulations are carried out for 2Tx-2Rx and 4Tx-2Rx antenna configurations. QPSK and 16-QAM constellations are used in the simulations. The 2Tx-2Rx system uses the 2-bit Grassmannian codebook ([Love & Heath (2003)]-TABLE II), and the 4Tx-2Rx system adopts the 4-bit codebook in 3GPP specification ([3GPP TS 36.211 (2009)]-Table 6.3.4.2.3-2).

Figure 2 and 3 show the average SER in uncorrelated Rayleigh fading. The SER bounds (31) (33) are tight in these figures.

We also consider a correlated Rayleigh fading channel. The channel correlation matrix $\mathbf{\Phi}^2$ is generated according to the 802.11n model D [Erceg et al. (2004)]. We assume uniform linear arrays with 0.5-wavelength adjacent antenna spacing, as in [Erceg et al. (2004), Section 7]. Figure 4 and 5 plot the average SER in this fading environment. In both figures, the gap between the simulation result and the bound (35) is no more than 2 dB. The conjectured SER formula (36) is even tighter than the bound.

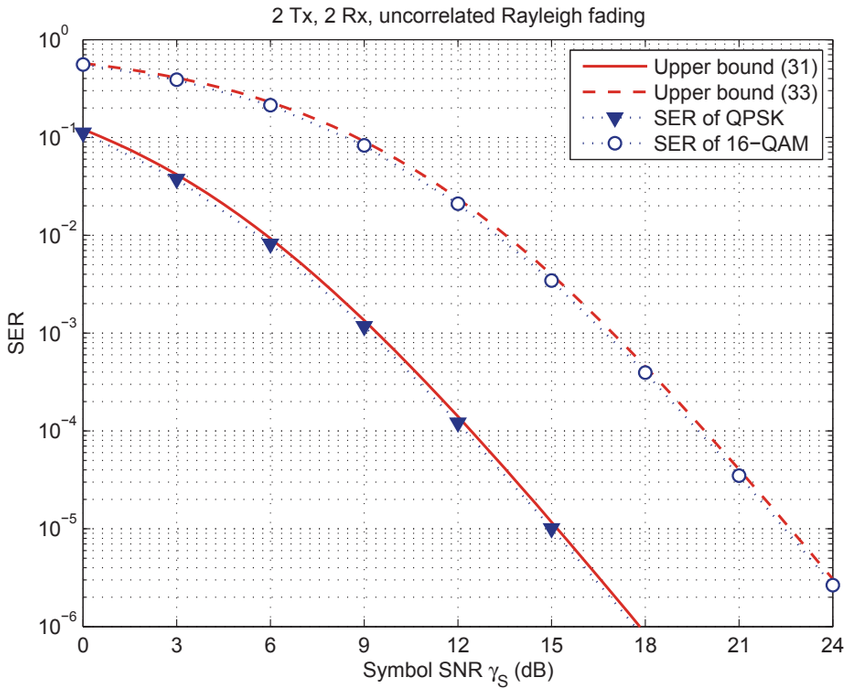

Fig. 2. SER of the 2Tx-2Rx beamforming system in Rayleigh fading environment.

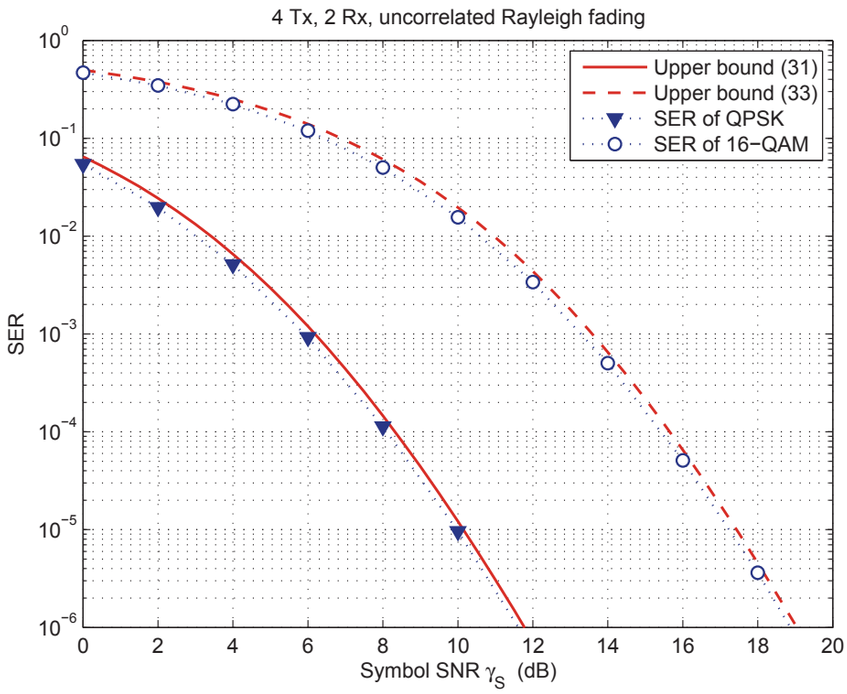

Fig. 3. SER of the 4Tx-2Rx beamforming system in Rayleigh fading environment.

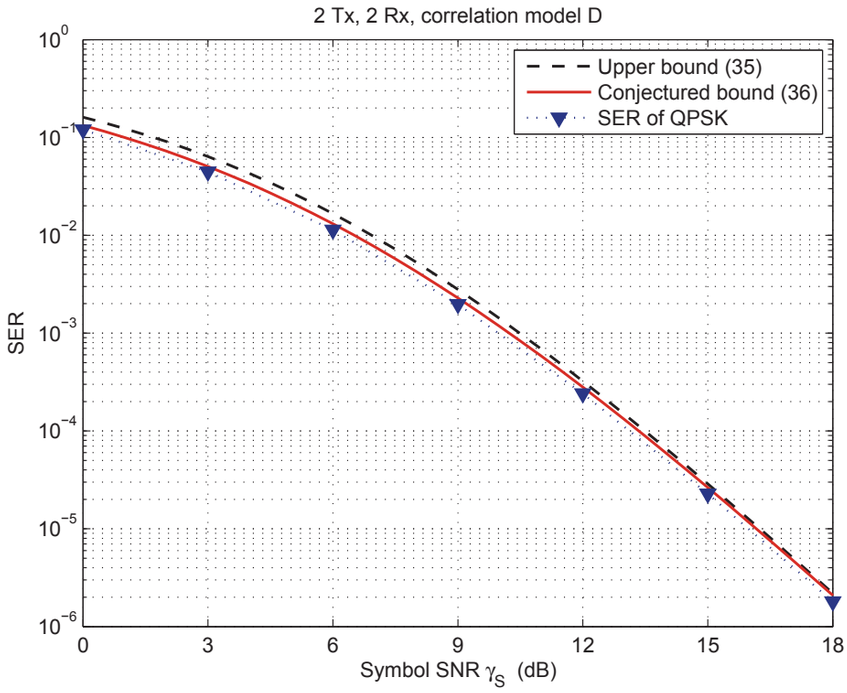

Fig. 4. SER of the 2Tx-2Rx beamforming system in correlated Rayleigh fading environment.

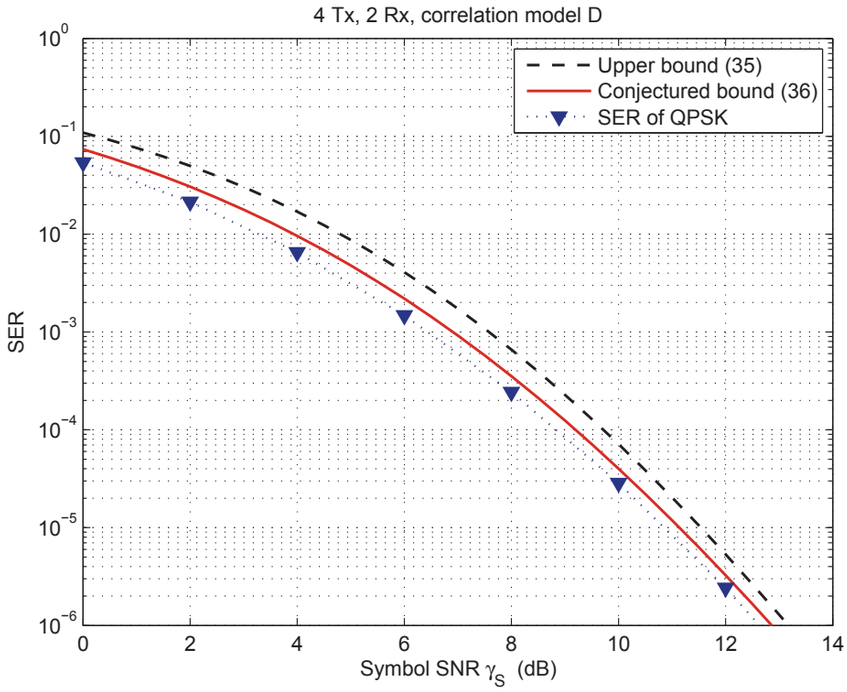

Fig. 5. SER of the 4Tx-2Rx beamforming system in correlated Rayleigh fading environment.

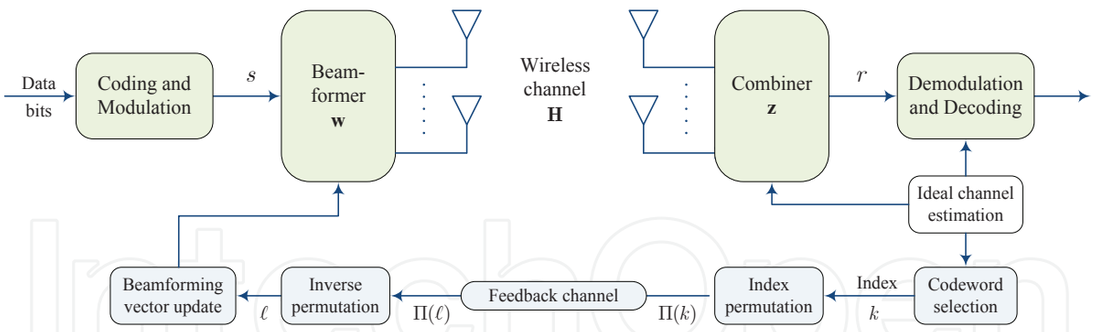

Fig. 6. A finite-rate beamforming system with index permutation.

3. Effect of feedback error and index assignment

In Section 2, the feedback link is assumed to be error-free, but feedback error is inevitable in practice. In this section, we study a finite-rate beamforming system with feedback error. It is shown that feedback error deteriorates not only the array gain but also the diversity gain. To mitigate the effect of feedback error, IA technique is adopted, which is popular in conventional VQ designs (see [Zeger & Gersho (1990)] [Ben-David & Malah (2005)] and references therein). IA technique is preferable to other error-protection methods, e.g. error-control coding, because it requires neither additional feedback bits nor additional signal processing, i.e. it is *redundancy-free*.

3.1 System model

The finite-rate beamforming system with feedback error is illustrated in Figure 6. The forward part of this system is similar to that in Section 2.1. The wireless channel is modeled as an $N_r \times N_t$ random matrix with i.i.d. $\mathcal{CN}(0,1)$ entries. The input-output of the forward part is given by

$$r = \mathbf{z}^* \mathbf{H} \mathbf{w} s + \mathbf{z}^* \boldsymbol{\eta}, \tag{37}$$

where

- $\mathbf{H}$ denotes the $N_r \times N_t$ channel matrix. Assuming i.i.d. Rayleigh fading, the entries of $\mathbf{H}$ are independent $\mathcal{CN}(0,1)$ random variables;
- $s \in \mathbb{C}$ is the information-bearing symbol;
- $\mathbf{w} \in \mathbb{C}^{N_t}$ stands for the unit-norm beamforming vector;
- $\mathbf{z} = \mathbf{Hw}/\|\mathbf{Hw}\|$ is the MRC combining vector;
- $\boldsymbol{\eta} \in \mathbb{C}^{N_r}$ refers to the noise vector with independent $\mathcal{CN}(0, N_0)$ entries;
- $r \in \mathbb{C}$ denotes the signal after receive combining.

The instantaneous receive SNR in (37) is given by

$$\gamma = \gamma_S \|\mathbf{Hw}\|^2, \tag{38}$$

where

$$\gamma_S \triangleq \mathbb{E}(|s|^2)/N_0 \tag{39}$$

is the average symbol SNR.

In the system, the beamforming vector $\mathbf{w}$ is determined by feedback information. The receiver conveys the feedback information to the transmitter via a low-rate feedback link, which

consists of the five blocks at the bottom of Figure 6. The 'Index permutation' and 'Inverse permutation' blocks are used to cope with feedback error. A codebook $\mathcal{C} = \{\mathbf{c}_1, \cdots, \mathbf{c}_{N_c}\}$ is designed in advance and stored at both the transmitter and the receiver. The codewords $\mathbf{c}_k$'s are unit-norm vector. The receiver selects the optimal codeword that maximize the instantaneous receive SNR, i.e.

$$\mathbf{c}_{\text{opt}} = \arg\max_{\mathbf{c}\in\mathcal{C}} \|\mathbf{Hc}\|^2. \tag{40}$$

If the codeword $\mathbf{c}_k$ is selected ($\mathbf{c}_{\text{opt}} = \mathbf{c}_k$), its index k is fed into the 'Index permutation' block, which performs permutation Π on this index and outputs $\Pi(k)$. The permutation Π is an invertible (one-to-one and onto) operator from the index set $\{1, \cdots, N_c\}$ to itself. For each index k, Π uniquely maps it to another index $\Pi(k) \in \{1, \cdots, N_c\}$. Given the codebook cardinality N_c, there are $N_c!$ permutations [Ben-David & Malah (2005)]. For example, when $N_c = 3$, one possible permutation is to map $1 \to 3$, $2 \to 1$, and $3 \to 2$, respectively.
The permutated index $\Pi(k)$ is then sent to the transmitter via the 'feedback channel', which is modeled as a discrete memoryless channel (DMC) with transition probability

$$T[i, j] = \Pr\{\text{DMC output is } j \,|\, \text{DMC input is } i\}, \qquad i, j = 1, \cdots, N_c. \tag{41}$$

Due to possible feedback error, the feedback channel does not always output the correct information. Supposing that the output of the feedback channel is $\Pi(\ell)$, the transmitter performs the inverse-permutation Π^{-1} on $\Pi(\ell)$ and obtains the index ℓ. The corresponding codeword $\mathbf{c}_\ell$ is used to update the beamforming vector. Conditioned on the optimal codeword $\mathbf{c}_{\text{opt}} = \mathbf{c}_k$, the probability that the transmitter uses $\mathbf{c}_\ell$ as the beamforming vector is given by

$$\begin{aligned}\Pr(\mathbf{w} = \mathbf{c}_\ell | \mathbf{c}_{\text{opt}} = \mathbf{c}_k) &= \Pr\left(\text{DMC output is } \Pi(\ell) \,|\, \text{DMC input is } \Pi(k)\right) \\ &= T[\Pi(k), \Pi(\ell)], \qquad k, \ell = 1, \cdots, N_c.\end{aligned} \tag{42}$$

Feedback error will deteriorate the performance of beamforming. In the following, we will quantify the effect of feedback error on the diversity gain and array gain.

3.2 The diversity gain

Diversity gain refers to the slope of SER-vs-SNR curve (on a log-log scale) as SNR approaches infinity. With error-free feedback, a well-designed beamformer can provide full diversity gain $N_t \times N_r$ if the codebook cardinality $N_c \geq N_t$ [Love & Heath (2005)]. However, the diversity gain may decrease to N_r due to feedback error, as shown in the following lemma.

Lemma 3. *For the beamforming system described in Section 3.1, the diversity gain equals to N_r, if the transition probability of the DMC feedback channel satisfies*

$$T[i, j] \geq T_{\min} > 0, \qquad i, j = 1, \cdots, N_c. \tag{43}$$

Proof: According to [Tse & Viswanath (2005)], the diversity gain is equal to

$$\lim_{\gamma_S \to \infty} -\frac{\log P_{\text{out}}}{\log \gamma_S}, \tag{44}$$

where P_{out} denotes the outage probability. For the beamforming system based on finite-rate feedback, the outage probability is given by [Mukkavilli et al. (2003); Mondal & Heath (2006)]

$$\begin{aligned}P_{\text{out}} &= \Pr\left(\log_2(1 + \gamma_S \|\mathbf{Hw}\|^2) < R\right) \\ &= \Pr\left(\|\mathbf{Hw}\|^2 < (2^R - 1)/\gamma_S\right),\end{aligned} \tag{45}$$

where R denotes the desired transmission rate. By the law of total probability, the right-hand-side of (45) can be expanded to give

$$\begin{aligned} P_{\text{out}} &= \sum_{k=1}^{N_c}\sum_{\ell=1}^{N_c} \Pr\left(\|\mathbf{H}\mathbf{c}_\ell\|^2 < \frac{2^R-1}{\gamma_S} \,\middle|\, \mathbf{c}_{\text{opt}} = \mathbf{c}_k \right) \Pr\left(\mathbf{w} = \mathbf{c}_\ell \,,\, \mathbf{c}_{\text{opt}} = \mathbf{c}_k\right) \\ &\overset{(42)}{=} \sum_{k=1}^{N_c}\sum_{\ell=1}^{N_c} \Pr\left(\|\mathbf{H}\mathbf{c}_\ell\|^2 < \frac{2^R-1}{\gamma_S} \,\middle|\, \mathbf{c}_{\text{opt}} = \mathbf{c}_k \right) T[\,\Pi(k), \Pi(\ell)]\, \Pr(\mathbf{c}_{\text{opt}} = \mathbf{c}_k) \\ &\overset{(43)}{\geq} T_{\min} \sum_{\ell=1}^{N_c}\sum_{k=1}^{N_c} \Pr\left(\|\mathbf{H}\mathbf{c}_\ell\|^2 < \frac{2^R-1}{\gamma_S} \,\middle|\, \mathbf{c}_{\text{opt}} = \mathbf{c}_k \right) \Pr(\mathbf{c}_{\text{opt}} = \mathbf{c}_k) \\ &= T_{\min} \sum_{\ell=1}^{N_c} \Pr\left(\|\mathbf{H}\mathbf{c}_\ell\|^2 < \frac{2^R-1}{\gamma_S} \right). \end{aligned} \tag{46}$$

Similarly, because $T[\,\Pi(k), \Pi(\ell)] \leq 1$ holds trivially, we have

$$P_{\text{out}} \leq \sum_{l=1}^{N_c} \Pr\left(\|\mathbf{H}\mathbf{c}_\ell\|^2 < \frac{2^R-1}{\gamma_S} \right). \tag{47}$$

Since the codeword $\mathbf{c}_\ell$ is deterministic and unit-norm, $\mathbf{H}\mathbf{c}_\ell$ is a Gaussian distributed random vector with zero mean and covariance $\mathbf{I}_{N_r}$. So $\|\mathbf{H}\mathbf{c}_\ell\|^2$ has a central chi-square distribution with $2N_r$ degrees of freedom. Hence

$$\Pr\left\{ \|\mathbf{H}\mathbf{c}_\ell\|^2 < \frac{2^R-1}{\gamma_S} \right\} = \underbrace{1 - \exp\left(-\frac{2^R-1}{\gamma_S}\right) \sum_{m=0}^{N_r-1} \frac{1}{m!} \left(\frac{2^R-1}{\gamma_S}\right)^m}_{\triangleq\, f(\gamma_S)}, \quad \forall\, \ell. \tag{48}$$

Substituting this equation into (46) and (47), one obtains

$$T_{\min} N_c\, f(\gamma_S) \leq P_{\text{out}} \leq N_c\, f(\gamma_S)\,.$$

Then, using the squeezing theorem, we get the diversity gain

$$\lim_{\gamma_S \to \infty} -\frac{\log P_{\text{out}}}{\log \gamma_S} = \lim_{\gamma_S \to \infty} -\frac{\log f(\gamma_S)}{\log \gamma_S} = N_r\,, \tag{49}$$

where the last equality can be derived by repeatedly applying L'Hospital's rule. This is the desired result. □

Two remarks about Lemma 3 are in order.

Remark 1 (BSC). The constraint (43) is satisfied by many DMC's. For example, binary symmetric channel (BSC) is an important DMC, whose transition probability is

$$T_{\text{BSC}}[i,j] = p^{\,d_{\text{H}}(i-1,j-1)} (1-p)^{B - d_{\text{H}}(i-1,j-1)} \qquad i,j = 1, \cdots, N_c, \tag{50}$$

where p is a parameter of the BSC; $N_c = 2^B$; and $d_{\text{H}}(i-1, j-1)$ denotes the Hamming distance between the binary representations of $i-1$ and $j-1$. The BSC satisfies (43) if $p > 0$. Hence, a beamforming system based on finite-rate feedback can only achieve a diversity gain of N_r, if the feedback channel is a BSC.

Remark 2(Comparison with STBC). With error-free feedback, finite-rate beamforming outperforms space-time block coding (STBC), because beamforming provides not only diversity gain but also array gain. However, this conclusion should be reconsidered if there exists feedback error. According to Lemma 1, a beamforming system based on finite-rate feedback may suffer from a large diversity gain loss due to feedback error. So at sufficiently high SNR, the performance of beamforming will be worse than that of STBC. The comparison at low-to-medium SNR is of practical importance, but out of the scope of this book.

3.3 The array gain

The array gain is defined as the ratio of the average receive SNR $\mathbb{E}\gamma$ and the symbol SNR γ_S. It reflects the increase in average receive SNR that arises from the coherent combining effect of multiple antennas.

Consider the case that the receiver selects $\mathbf{c}_k$ as the optimal codeword, but the transmitter uses $\mathbf{c}_\ell$ as the beamforming vector due to feedback error. The average receive SNR conditioned on this case is

$$\gamma_S \, \mathbb{E}\big(\|\mathbf{H}\mathbf{c}_\ell\|^2 \,\big|\, \mathbf{c}_{\text{opt}} = \mathbf{c}_k\big) = \gamma_S \, \mathbf{c}_\ell^* \, \mathbb{E}(\mathbf{H}^*\mathbf{H}|\mathbf{c}_{\text{opt}} = \mathbf{c}_k) \, \mathbf{c}_\ell \, .$$

Therefore, by the law of total expectation, the array gain can be written as

$$\begin{aligned}\frac{\mathbb{E}(\gamma)}{\gamma_S} &= \sum_{k=1}^{N_c} \sum_{\ell=1}^{N_c} \mathbf{c}_\ell^* \, \mathbb{E}\left(\mathbf{H}^*\mathbf{H} \,\middle|\, \mathbf{c}_{\text{opt}} = \mathbf{c}_k\right) \mathbf{c}_\ell \, \Pr\left(\mathbf{w} = \mathbf{c}_\ell \, , \, \mathbf{c}_{\text{opt}} = \mathbf{c}_k\right) \\ &\overset{(42)}{=} \sum_{k=1}^{N_c} \sum_{\ell=1}^{N_c} \mathbf{c}_\ell^* \, \mathbb{E}\left(\mathbf{H}^*\mathbf{H} \,\middle|\, \mathbf{c}_{\text{opt}} = \mathbf{c}_k\right) \mathbf{c}_\ell \, T[\,\Pi(k), \Pi(l)] \, \Pr(\mathbf{c}_{\text{opt}} = \mathbf{c}_k). \end{aligned} \tag{51}$$

In the right-hand-side of (51), the accurate values of $\mathbb{E}\left(\mathbf{H}^*\mathbf{H}|\mathbf{c}_{\text{opt}} = \mathbf{c}_k\right)$ and $\Pr(\mathbf{c}_{\text{opt}} = \mathbf{c}_k)$ are hard to obtain, but their approximations can be derived as follows.

Since the channel matrix $\mathbf{H}$ has independent $\mathcal{CN}(0,1)$ entries, $\mathbf{H}^*\mathbf{H}$ is Wishart distributed. Its eigen-decomposition is denoted as

$$\mathbf{H}^*\mathbf{H} = \left[\mathbf{u}_1, \cdots, \mathbf{u}_{N_t}\right] \begin{bmatrix} \lambda_1 & & \\ & \ddots & \\ & & \lambda_{N_t} \end{bmatrix} \begin{bmatrix} \mathbf{u}_1^* \\ \vdots \\ \mathbf{u}_{N_t}^* \end{bmatrix} = \sum_{n=1}^{N_t} \lambda_n \mathbf{u}_n \mathbf{u}_n^* \tag{52}$$

where $\lambda_1 \geq \cdots \geq \lambda_{N_t} \geq 0$ and $\mathbf{u}_1, \cdots, \mathbf{u}_{N_t}$ denote the eigenvalues and the eigenvectors, respectively. The distribution of nonzero eigenvalues is known. The eigen matrix $\mathbf{U} = \left[\mathbf{u}_1, \cdots, \mathbf{u}_{N_t}\right]$ is uniformly distributed on the group of $N_t \times N_t$ unitary matrices and *independent of the eigenvalues* [Love & Heath (2003), Lemma 1].

If the feedback channel is perfect, the transmitter uses the eigenvector $\mathbf{u}_1$ as the beamforming vector, which is called maximum ratio transmission (MRT). But this is not the case in practice, where the quantized information — the optimal codeword $\mathbf{c}_{\text{opt}}$ — is fed back to the transmitter. Then, one would expect that the ideal feedback information $\mathbf{u}_1$ and the quantized version $\mathbf{c}_{\text{opt}}$ are 'close'. Since both $\mathbf{u}_1$ and $\mathbf{c}_{\text{opt}}$ belong to the unit hypersphere

$$\Omega^{N_t} \triangleq \{\mathbf{x} \in \mathbb{C}^{N_t} : \mathbf{x}^*\mathbf{x} = 1\}, \tag{53}$$

a suitable measure of their 'closeness' is the chordal distance, defined as

$$d_{\text{c}}(\mathbf{x}_1, \mathbf{x}_2) = \sqrt{1 - |\mathbf{x}_1^*\mathbf{x}_2|^2}, \qquad \mathbf{x}_1, \mathbf{x}_2 \in \Omega^{N_t}. \tag{54}$$

Now define a spherical cap centered at the codeword $\mathbf{c}_k$ as

$$\begin{aligned}\mathcal{S}(\mathbf{c}_k) &= \left\{\mathbf{x} \in \Omega^{N_t} : d_{\mathrm{c}}(\mathbf{x}, \mathbf{c}_k) < \sqrt{\alpha}\right\} \\ &= \left\{\mathbf{x} \in \Omega^{N_t} : |\mathbf{x}^* \mathbf{c}_k|^2 > 1 - \alpha\right\}, \quad k = 1, \cdots, N_c. \end{aligned} \tag{55}$$

We use the event $\{\mathbf{u}_1 \in \mathcal{S}(\mathbf{c}_k)\}$ to approximate the event $\{\mathbf{c}_{\mathrm{opt}} = \mathbf{c}_k\}$, which leads to the following approximations

$$\mathbb{E}\left(\mathbf{H}^*\mathbf{H} \,|\, \mathbf{c}_{\mathrm{opt}} = \mathbf{c}_k\right) \simeq \mathbb{E}\left\{\mathbf{H}^*\mathbf{H} \,|\, \mathbf{u}_1 \in \mathcal{S}(\mathbf{c}_k)\right\} \overset{(52)}{=} \sum_{n=1}^{N_t} \mathbb{E}(\lambda_n)\, \mathbb{E}\{\mathbf{u}_n \mathbf{u}_n^* \,|\, \mathbf{u}_1 \in \mathcal{S}(\mathbf{c}_k)\}, \tag{56}$$

$$\Pr(\mathbf{c}_{\mathrm{opt}} = \mathbf{c}_k) \simeq \Pr\left\{\mathbf{u}_1 \in \mathcal{S}(\mathbf{c}_k)\right\}. \tag{57}$$

In order to simplify the right-hand-side of (56), we derive the following result.

Lemma 4. *If* $\mathbf{U} = [\mathbf{u}_1, \cdots, \mathbf{u}_{N_t}]$ *is uniformly distributed on the group of* $N_t \times N_t$ *unitary matrices, then*

$$\mathbb{E}\left\{\mathbf{u}_1 \mathbf{u}_1^* \,|\, \mathbf{u}_1 \in \mathcal{S}(\mathbf{c}_k)\right\} = \frac{\alpha}{N_t}\mathbf{I}_{N_t} + (1-\alpha)\,\mathbf{c}_k \mathbf{c}_k^*, \quad k = 1, \cdots, N_c; \tag{58}$$

$$\begin{aligned}\mathbb{E}\left\{\mathbf{u}_n \mathbf{u}_n^* \,|\, \mathbf{u}_1 \in \mathcal{S}(\mathbf{c}_k)\right\} = \frac{N_t - \alpha}{N_t(N_t-1)}\,\mathbf{I}_{N_t} - \frac{1-\alpha}{N_t - 1}\,\mathbf{c}_k \mathbf{c}_k^*, \\ n = 2, \cdots, N_t,\ k = 1, \cdots, N_c. \end{aligned} \tag{59}$$

Proof: Since $\mathbf{U}$ is uniformly distributed, $\mathbf{u}_1$ is uniformly distributed on the unit hypersphere Ω^{N_t}. Conditioned on a particular realization of $\mathbf{u}_1$, $\mathbf{u}_n, n = 2, \cdots, N_t$, is uniformly distributed on the set [Marzetta & Hochwald (1999)]

$$\mathcal{O}(\mathbf{u}_1) = \{\mathbf{u}_n \in \Omega^{N_t} : \mathbf{u}_n^* \mathbf{u}_1 = 0\}.$$

Therefore

$$\mathbb{E}\left\{\mathbf{u}_1 \mathbf{u}_1^* \,|\, \mathbf{u}_1 \in \mathcal{S}(\mathbf{c}_k)\right\} = \int_{\mathcal{S}(\mathbf{c}_k)} C_0\, \mathbf{u}_1 \mathbf{u}_1^* \mathrm{d}\mathbf{u}_1, \tag{60}$$

$$\mathbb{E}\left\{\mathbf{u}_n \mathbf{u}_n^* \,|\, \mathbf{u}_1 \in \mathcal{S}(\mathbf{c}_k)\right\} = \int_{\mathcal{S}(\mathbf{c}_k)} C_0 \left(\int_{\mathcal{O}(\mathbf{u}_1)} C_1\, \mathbf{u}_n \mathbf{u}_n^* \mathrm{d}\mathbf{u}_n\right) d\mathbf{u}_1, \quad n = 2, \cdots, N_t, \tag{61}$$

where

$$C_0 = \frac{(N_t - 1)!}{2\pi^{N_t} \alpha^{N_t - 1}}, \qquad C_1 = \frac{(N_t - 2)!}{2\pi^{N_t - 1}}, \tag{62}$$

such that

$$\int_{\mathcal{S}(\mathbf{c}_k)} C_0\, \mathrm{d}\mathbf{u}_1 = 1, \qquad \int_{\mathcal{O}(\mathbf{u}_1)} C_1\, \mathrm{d}\mathbf{u}_n = 1.$$

The calculation of (60). Let $\mathbf{\Theta} = [\mathbf{c}_k, \mathbf{\Theta}_0]$ be a unitary matrix, where $\mathbf{\Theta}_0$ is chosen arbitrarily with the constraint that $\mathbf{\Theta}$ is unitary. Using the transformation $\mathbf{v} = \mathbf{\Theta}^* \mathbf{u}_1$, $\mathcal{S}(\mathbf{c}_k)$ is rotated to

$$\mathcal{S}(\mathbf{e}_1) = \{\mathbf{x} \in \Omega^{N_t} : |\mathbf{x}^* \mathbf{e}_1|^2 > 1 - \alpha\},$$

where $\mathbf{e}_1 \triangleq [1, 0, \cdots, 0]^T$. The Jacobian of this transformation is 1, because $\mathbf{\Theta}$ is unitary. Hence, applying the transformation $\mathbf{v} = \mathbf{\Theta}^* \mathbf{u}_1$ to the right-hand-side of (60) gives

$$\mathbb{E}\left\{\mathbf{u}_1 \mathbf{u}_1^* \,|\, \mathbf{u}_1 \in \mathcal{S}(\mathbf{c}_k)\right\} = \int_{\mathcal{S}(\mathbf{e}_1)} C_0 \mathbf{\Theta} \mathbf{v}\mathbf{v}^* \mathbf{\Theta}^* \mathrm{d}\mathbf{v} = \mathbf{\Theta}\left(C_0 \int_{\mathcal{S}(\mathbf{e}_1)} \mathbf{v}\mathbf{v}^* \mathrm{d}\mathbf{v}\right)\mathbf{\Theta}^*. \tag{63}$$

The surface integration $\int_{\mathcal{S}(\mathbf{e}_1)} \mathbf{v}\mathbf{v}^* \mathrm{d}\mathbf{v}$ can be converted to $2N_t - 1$ dimensional multiple integration [Fleming (1977)]. Let

$$\mathcal{G} = \left\{\mathbf{y} \in \mathbb{R}^{2N_t - 1} : -\pi < y_1 < \pi,\ y_2^2 + \cdots + y_{2N_t-1}^2 < \alpha\right\}. \tag{64}$$

Construct the transformation $\mathbf{g} : \mathcal{G} \to \mathcal{S}(\mathbf{e}_1)$

$$\begin{cases} \Re(v_1) = g_1(\mathbf{y}) = \sqrt{1 - y_2^2 - \cdots - y_{2N_t-1}^2}\, \cos y_1\,, \\ \Im(v_1) = g_2(\mathbf{y}) = \sqrt{1 - y_2^2 - \cdots - y_{2N_t-1}^2}\, \sin y_1\,, \\ \Re(v_n) = g_{2n-1}(\mathbf{y}) = y_{2n-2}, \qquad n = 2, \cdots, N_t\,, \\ \Im(v_n) = g_{2n}(\mathbf{y}) = y_{2n-1}, \qquad n = 2, \cdots, N_t\,, \end{cases} \tag{65}$$

where $\Re(v_n)$ and $\Im(v_n)$ denote the real and imaginary parts of the nth entry of $\mathbf{v}$ respectively. It can be verified that

$$\mathcal{J}\mathbf{g} \triangleq \sqrt{\det\left[(D\mathbf{g})^T (D\mathbf{g})\right]} \;=\; 1\,, \tag{66}$$

where $D\mathbf{g}$ denotes the $2N_t \times (2N_t - 1)$ differential matrix. The (i, j)-th entry of $D\mathbf{g}$ is given by

$$[D\mathbf{g}]_{i,j} = \frac{\partial g_i}{\partial y_j}, \quad i = 1, \cdots, 2N_t,\ j = 1, \cdots, 2N_t - 1.$$

Then, under the transformation $\mathbf{v} = \mathbf{g}(\mathbf{y})$,

$$\begin{aligned} \left[\int_{\mathcal{S}(\mathbf{e}_1)} \mathbf{v}\mathbf{v}^* \mathrm{d}\mathbf{v}\right]_{n,\ell} &= \int_{\mathcal{S}(\mathbf{e}_1)} \left[\Re(v_n)\Re(v_\ell) + \Im(v_n)\Im(v_\ell)\right] + j\left[\Im(v_n)\Re(v_\ell) - \Re(v_n)\Im(v_\ell)\right] \mathrm{d}\mathbf{v} \\ &= \int_{\mathcal{G}} \Big(\left[g_{2n-1}\, g_{2l-1} + g_{2n}\, g_{2l}\right] + j\left[g_{2n}\, g_{2l-1} - g_{2n-1}\, g_{2l}\right]\Big)\, \mathcal{J}\mathbf{g}\, \mathrm{d}\mathbf{y} \\ &= \int_{\mathcal{G}} g_{2n-1}\, g_{2l-1}\, \mathrm{d}\mathbf{y} + \int_{\mathcal{G}} g_{2n}\, g_{2l}\, \mathrm{d}\mathbf{y} + j\left(\int_{\mathcal{G}} g_{2n}\, g_{2l-1}\, \mathrm{d}\mathbf{y} - \int_{\mathcal{G}} g_{2n-1}\, g_{2l}\, \mathrm{d}\mathbf{y}\right) \end{aligned}$$

The calculation of these integrations is straightforward, e.g.

$$\int_{\mathcal{G}} g_3\, g_3 \mathrm{d}\mathbf{y} = \int_{\mathcal{G}} y_2^2\, \mathrm{d}\mathbf{y} = \int_{-\pi}^{\pi} \mathrm{d}y_1 \int_{y_2^2 + \cdots + y_{2N_t-1}^2 < \alpha} y_2^2\, \mathrm{d}y_2 \cdots \mathrm{d}y_{2N_t-1} = \frac{\pi \alpha^{N_t}}{N_t!}\,.$$

Collecting the results, one obtains

$$C_0 \int_{\mathcal{S}(\mathbf{e}_1)} \mathbf{v}\mathbf{v}^* \mathrm{d}\mathbf{v} = \frac{\alpha}{N_t}\, \mathbf{I}_{N_t} + (1 - \alpha)\, \mathbf{e}_1 \mathbf{e}_1^*\,. \tag{67}$$

Substituting (67) into (63), we get (58).

The calculation of (61) . The derivation of the inner integration in the right-hand-side of (61) is along the line of the calculation of (60). So it is omitted here. The result is

$$\int_{\mathcal{O}(\mathbf{u}_1)} C_1 \mathbf{u}_n \mathbf{u}_n^* \, \mathrm{d}\mathbf{u}_n = \frac{1}{N_t - 1} \left(\mathbf{I}_{N_t} - \mathbf{u}_1 \mathbf{u}_1^* \right). \tag{68}$$

Substituting this into (61) yields

$$\begin{aligned} \mathbb{E}\left\{ \mathbf{u}_n \mathbf{u}_n^* \,|\, \mathbf{u}_1 \in \mathcal{S}(\mathbf{c}_k) \right\} &= \frac{C_0}{N_t - 1} \int_{\mathcal{S}(\mathbf{c}_k)} \mathbf{I}_{N_t} \mathrm{d}\mathbf{u}_1 - \frac{C_0}{N_t - 1} \int_{\mathcal{S}(\mathbf{c}_k)} \mathbf{u}_1 \mathbf{u}_1^* \mathrm{d}\mathbf{u}_1 \\ &= \frac{N_t - \alpha}{N_t (N_t - 1)} \mathbf{I}_{N_t} - \frac{1 - \alpha}{N_t - 1} \mathbf{c}_k \mathbf{c}_k^*, \end{aligned}$$

which is the desired result (59). □

Applying Lemma 4 to (56) and using the fact

$$\sum_{n=1}^{N_t} \mathbb{E}(\lambda_n) = \mathbb{E}(\|\mathbf{H}\|_{\mathrm{F}}^2) = N_t N_r,$$

we obtain

$$\mathbb{E}\left(\mathbf{H}^* \mathbf{H} \,|\, \mathbf{c}_{\mathrm{opt}} = \mathbf{c}_k \right) \simeq \frac{N_t (1 - \alpha)}{N_t - 1} \Big(\mathbb{E}(\lambda_1) - N_r \Big) \mathbf{c}_k \mathbf{c}_k^* + \left(\frac{N_r (N_t - \alpha)}{N_t - 1} - \frac{1 - \alpha}{N_t - 1} \mathbb{E}(\lambda_1) \right) \mathbf{I}_{N_t} \qquad k = 1, \cdots, N_c. \tag{69}$$

Moreover, according to the results in [Mukkavilli et al. (2003)], the right-hand-side of (57) can be simplified as

$$\Pr(\mathbf{c}_{\mathrm{opt}} = \mathbf{c}_k) \simeq \Pr\left\{ \mathbf{u}_1 \in \mathcal{S}(\mathbf{c}_k) \right\} = \alpha^{N_t - 1}, \quad k = 1, \cdots, N_c \,. \tag{70}$$

The calculation is straightforward, and omitted here. To consist with

$$\sum_{k=1}^{N_c} \Pr(\mathbf{c}_{\mathrm{opt}} = \mathbf{c}_k) = 1,$$

we set

$$\alpha = \left(1 / N_c \right)^{\frac{1}{N_t - 1}}.$$

Substituting (69) and (70) into (51), the array gain of the beamforming system can be approximated by

$$\begin{aligned} \frac{\mathbb{E}(\gamma)}{\gamma_S} \simeq & \frac{N_r (N_t - \alpha)}{N_t - 1} - \frac{1 - \alpha}{N_t - 1} \mathbb{E}(\lambda_1) \\ & + \frac{N_t (1 - \alpha)}{N_c (N_t - 1)} \Big(\mathbb{E}(\lambda_1) - N_r \Big) \sum_{k=1}^{N_c} \sum_{\ell=1}^{N_c} |\mathbf{c}_k^* \mathbf{c}_\ell|^2 \, T[\,\Pi(k), \Pi(l)], \end{aligned} \tag{71}$$

which is the main result about the array gain.
We note that, in general, $\mathbb{E}(\lambda_1)$ can be obtained by numerical integration or simulation. It has closed-form expressions in some cases. In MISO systems, $\mathbf{H}$ reduces to a vector $\mathbf{h}$. Therefore

$$\mathbb{E}(\lambda_1) = \mathbb{E}(\|\mathbf{h}\|^2) = N_t, \qquad \text{when} \quad N_r = 1. \tag{72}$$

If $\min(N_t, N_r) = 2$, a closed form expression of $\mathbb{E}(\lambda_1)$ is derived in [Kang & Alouini (2004)]. As a special case, when the feedback is error-free, we have $T[\,i, j\,] = \delta_{i,j}$. In this case, (71) reduces to the result in [Mondal & Heath (2006)].

3.4 The index assignment

In the beamforming system, the adopted IA scheme Π affects the behavior of the feedback of the codeword index, which in turn impacts on the overall system performance. In this section, we focus on the design of the IA scheme, using the array gain (or equivalently, the average receive SNR) as a design metric.

According to (71), an IA scheme Π that maximizes the array gain can be obtained by solving

$$\begin{aligned} \underset{\Pi}{\text{maximize}} \ : \ & \sum_{k=1}^{N_c} \sum_{\ell=1}^{N_c} |\mathbf{c}_k^* \mathbf{c}_\ell|^2 \, T[\Pi(k), \Pi(\ell)] \\ \text{subject to} : \ & \Pi \text{ is a permutation} \end{aligned} \tag{73}$$

Maximization of the cost function in (73) over all of the $N_c!$ possible permutations is a special case of the quadratic assignment problem (QAP), and is known to be NP-complete. If N_c is small, it can be solved by brute-force search. But for a large codebook, e.g. $N_c \geq 16$, brute-force search is prohibitive since $16! > 10^{13}$, and suboptimal methods have been proposed in the literature [Zeger & Gersho (1990); Ben-David & Malah (2005)].

BSC is an important case of DMC. The optimization problem (73) can be simplified in the case of BSC feedback channel. In practice, feedback errors seldom occur, and the effect of multiple bit errors can be neglected. So the transition probability (50) can be approximated by

$$T_{\text{BSC}}[i,j] \simeq T_{\text{AP}}[i,j] = \begin{cases} (1-p)^B, & d_{\text{H}}(i-1, j-1) = 0; \\ p(1-p)^{B-1}, & d_{\text{H}}(i-1, j-1) = 1; \\ 0\,, & d_{\text{H}}(i-1, j-1) \geq 2, \end{cases} \tag{74}$$

and (73) can be simplified to

$$\begin{aligned} \underset{\Pi}{\text{maximize}} \ : \ & \sum_{k=1}^{N_c} \sum_{\ell=1}^{N_c} |\mathbf{c}_k^* \mathbf{c}_\ell|^2 \, T_{\text{AP}}[\Pi(k), \Pi(\ell)] \\ \text{subject to} : \ & \Pi \text{ is a permutation} \end{aligned} \tag{75}$$

The advantage of (75) is two-fold. 1) The computational complexity of the cost function is reduced, since most of T_{AP}'s are zero. 2) Its solution doesn't depend on the parameter p of the BSC [Zeger & Gersho (1990)]. Once we solve (75) for a particular value of p, the solution is valid for other values.

3.5 Numerical results

Simulations are carried out in (2,1,8) and (4,2,64) systems, where (N_t, N_r, N_c) denotes a system with N_t transmit antennas, N_r receive antennas, and codebook cardinality N_c. A BSC feedback channel is adopted in the simulations, Codebooks are downloaded from [Love's webpage (2006)]. We design good IA's for these codebooks by solving the simplified problem (75). To study the worst-case performance, bad IA's are also designed by minimizing the cost function of (75). The IA's of the (2,1,8) system are obtained by brute-force search, and shown in Table 1. The IA's of the (4,2,64) system are designed using the binary switching algorithm [Zeger & Gersho (1990)].

From the IA results in Table 1, we can gain an insight into how the good IA improves the system performance. For example, the first codeword is closest (with respect to the chordal distance) to the last codeword. The Hamming distance between their original indexes (1 and 8 respectively) is 3, while the Hamming distance between their good indexes (7 and

Codeword	Original IA, k	Good IA, $\Pi_{\text{good}}(k)$	Bad IA, $\Pi_{\text{bad}}(k)$
$[0.8393 - j\,0.2939,\ -0.1677 + j\,0.4256]^T$	1	7	1
$[-0.3427 + j\,0.9161,\ 0.0498 + j\,0.2019]^T$	2	1	4
$[-0.2065 + j\,0.3371,\ 0.9166 + j\,0.0600]^T$	3	6	2
$[0.3478 - j\,0.3351,\ 0.2584 + j\,0.8366]^T$	4	8	8
$[0.1049 + j\,0.6820,\ 0.6537 + j\,0.3106]^T$	5	2	5
$[0.0347 - j\,0.2716,\ 0.0935 - j\,0.9572]^T$	6	4	3
$[-0.7457 + j\,0.1181, -0.4553 - j\,0.4719]^T$	7	3	6
$[-0.7983 + j\,0.3232,\ 0.5000 + j\,0.0906]^T$	8	5	7

Table 1. Index assignment schemes for a 3-bit codebook

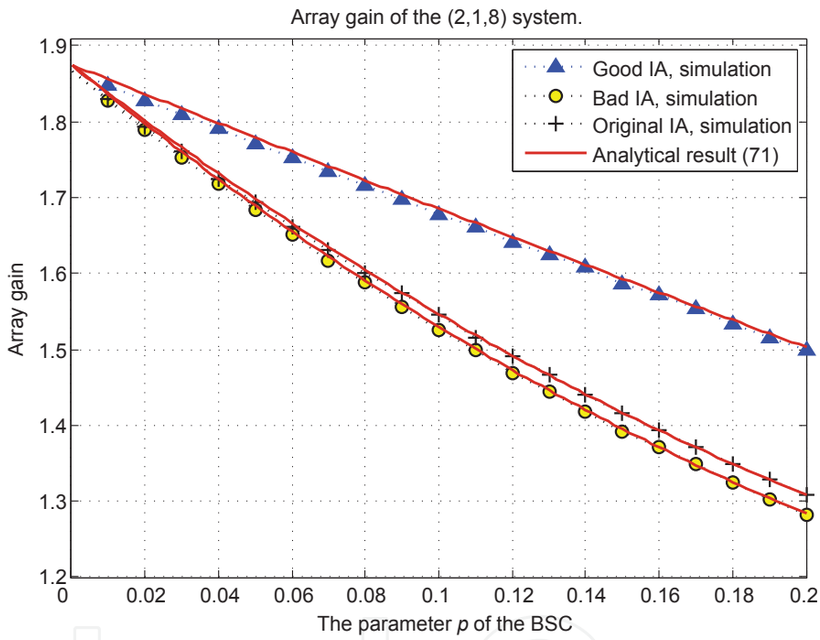

Fig. 7. The array gain of the (2,1,8) system.

5 respectively) is 1. Similarly, the second codeword is closest to the fifth codeword. The Hamming distance between their original indexes (2 and 5) is 2, and that between their good indexes (1 and 2) is 1. It is shown from these examples that the good IA scheme has assigned close indexes (in term of Hamming distance) to close codewords (in term of chordal distance). Figure 7 and 8 show the variation of the array gain with the increase of p. In the simulations, the SNR is fixed at $\gamma_S = 10$ dB. As shown in both figures, the good IA always outperforms the bad IA and the original IA. Furthermore, we can see that the analytical result (71) is tight. Figure 9 and 10 depict the SER simulation results. QPSK and 16-QAM modulations are used in (2,1,8) and (4,2,64) systems respectively. In the simulations, thirty-six symbols are transmitted in a block, and ideal coherent detection is adopted. In Figure 9, the SER of 'good IA' is much lower than that of 'bad IA', and approaches that of 'error-free feedback'. In Figure 10, the good IA outperforms the bad IA, though it cannot reach the performance of error-free feedback. In

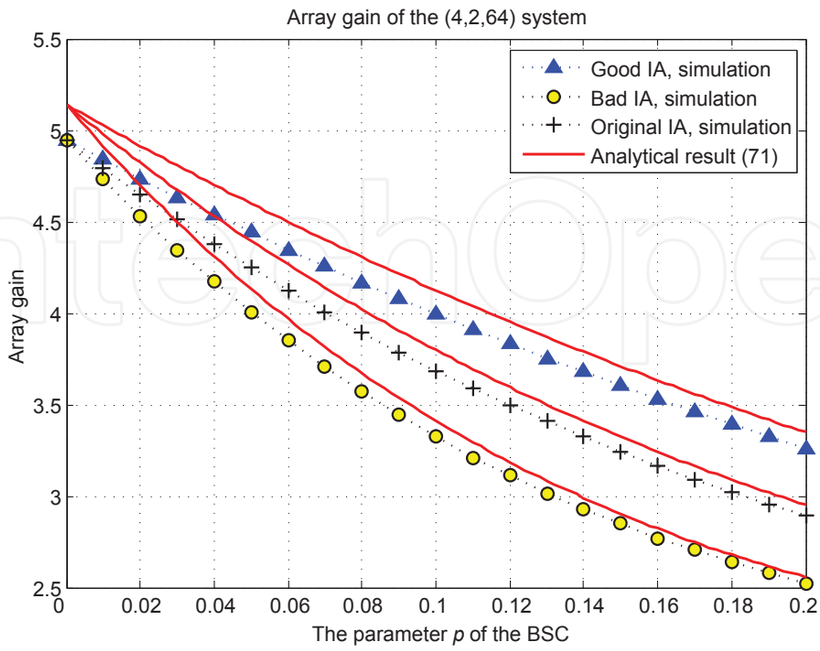

Fig. 8. The array gain of the (4,2,64) system.

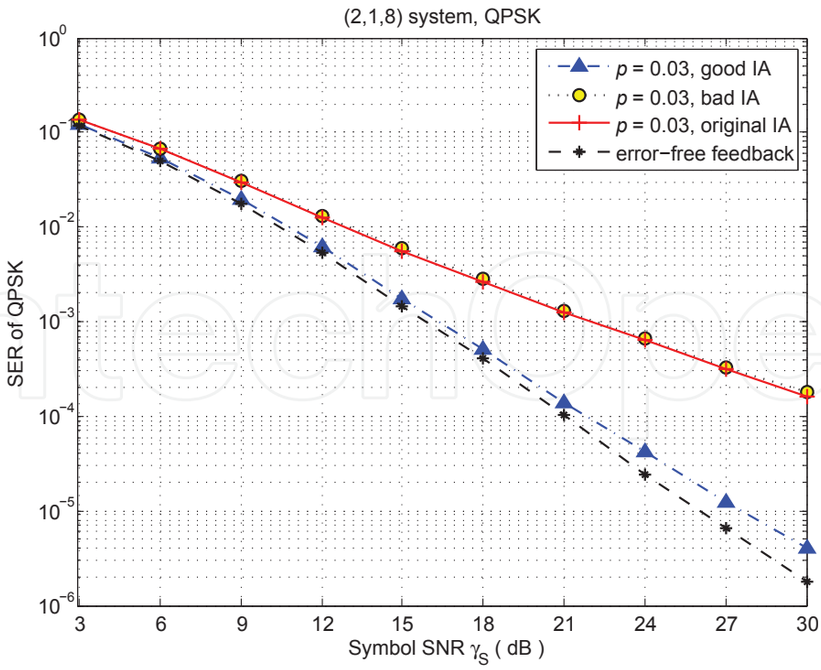

Fig. 9. SER of QPSK in the (2,1,8) system.

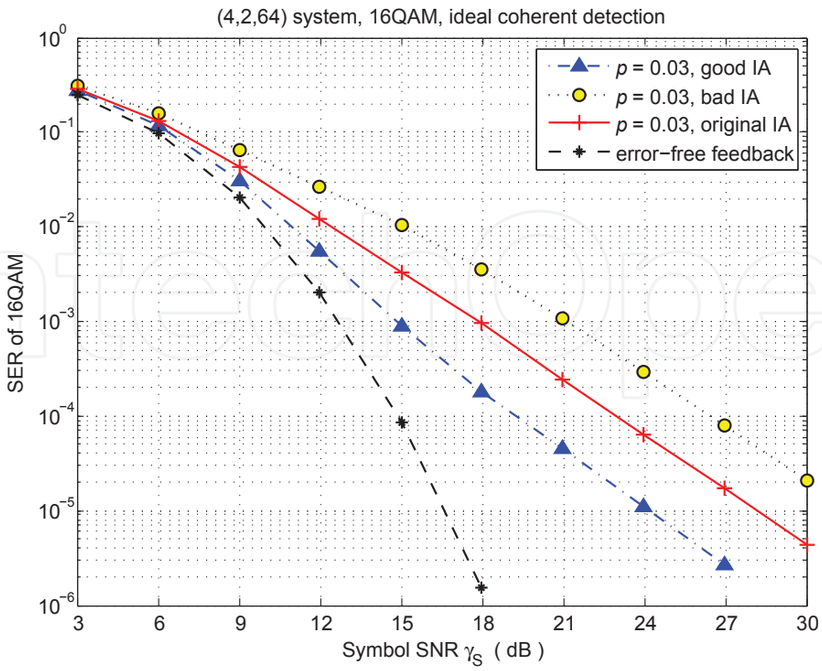

Fig. 10. SER of 16-QAM in the (4,2,64) system.

this case, IA technique shows its limitation. Other technique, such as error-control coding and automatic repeat-request (ARQ), is required to further compensate the performance degradation caused by feedback errors.
Moreover, it is observed from Figure 9 and 10 that the diversity gain (the slope of SER curve at high SNR) fits well with the conclusion of Lemma 3, except that the diversity gain of (2,1,8) system with good IA is not clear because the SNR is not large enough.

4. Effect of feedback delay and channel prediction

Feedback delay is harmful to a beamforming system based on finite-rate feedback, resulting in significant capacity loss [Huang et al. (2006)] and error-performance degradation [Ma & Zhang (2007)]. As an effective countermeasure against the feedback delay, channel prediction has been used in beamforming systems [Zhou & Giannakis (2004); Ma et al. (2008)]. For example, the minimum mean square error (MMSE) channel predictor was used in the predictive feedback scheme proposed in [11], where the authors analyzed the joint effect of imperfect channel estimation and feedback delay on the capacity of a beamforming system based on finite-rate feedback.

4.1 System model

Consider a beamforming system with N_t transmit and N_r receive antennas, as shown in Figure 11. The wireless channel is frequency-flat, and its temporal variation is slow enough to be considered quasi-static within some time interval T_B (called a block). Let $h_{m,n}(j)$ denote the fading coefficient of the (m,n)th channel branch (between transmit antenna n and receive antenna m) at block j. The fading coefficients are assumed to be zero-mean and jointly Gaussian. The channel is spatially white and temporally correlated according to Jakes' model,

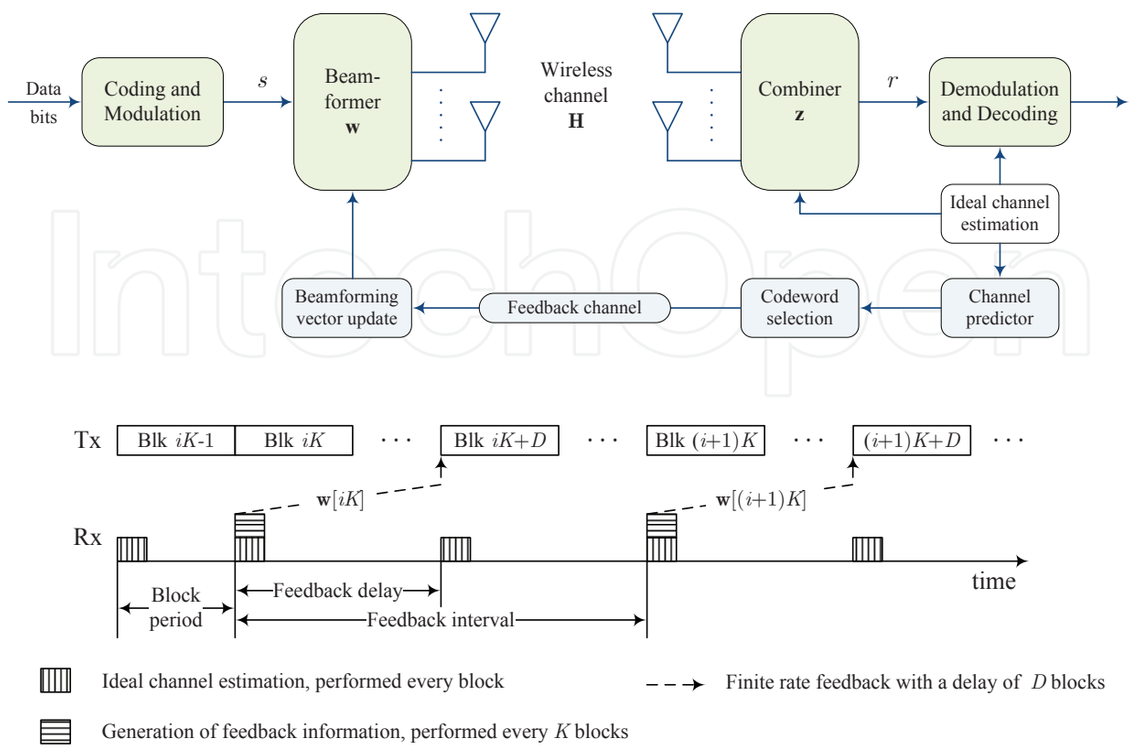

Fig. 11. A finite-rate beamforming system with channel prediction. (Top: system model. Bottom: frame structure.)

that is,

$$\mathbb{E}\{h_{m,n}(j)h^*_{m',n'}(j')\} = \begin{cases} J_0(2\pi f_d T_B|j-j'|), & m=m' \text{ and } n=n', \\ 0, & \text{else}, \end{cases} \tag{76}$$

where f_d denotes the Doppler spread; and $J_0(\cdot)$ is the zeroth-order Bessel function of the first kind. The channel coefficients at block j are collected into the $N_r \times N_t$ matrix $\mathbf{H}(j)$. We further assume that the receiver performs channel estimation at every block, and the estimation is perfect.

The frame structure is illustrated in the bottom of Figure 11. The system adopts a codebook based feedback scheme. A B-bit beamforming codebook $\mathcal{C} = \{\mathbf{c}_1, \cdots, \mathbf{c}_{N_c}\}$ is designed in advance, where $\mathbf{c}_1, \cdots, \mathbf{c}_{N_c} \in \mathbb{C}^{N_t}$ are *unit-norm* codewords and $N_c = 2^B$ In each feedback, the receiver selects a favorable codeword from the codebook and feeds back a B-bit codeword index to the transmitter. The feedback link is error-free, but has a delay of D blocks. Moreover, the feedback is carried out every K blocks, so that the average feedback rate $B/(KT_B)$ bps satisfies the feedback rate constraint.

The process of the ith feedback is described as follows. At block iK, the receiver predicts the MIMO channel, using a Pth order linear predictor. The predictor buffers the latest $P+1$ channel realizations $\mathbf{H}(iK), \cdots, \mathbf{H}(iK-P)$, and calculates the channel prediction according to

$$\widehat{\mathbf{H}}[iK] = \sum_{p=0}^{P} a^*(p)\mathbf{H}(iK-p), \tag{77}$$

where $\mathbf{a} \triangleq [a(0), \cdots, a(P)]^T$ is the predictor coefficient vector. The prediction is passed to the quantizer, which selects a favorable codeword from the beamforming codebook

$$\mathbf{w}[iK] = \arg\max_{\mathbf{c}\in\mathcal{C}} \left\|\widehat{\mathbf{H}}[iK]\mathbf{c}\right\|^2. \tag{78}$$

The index of $\mathbf{w}[iK]$ is sent to the transmitter via the feedback link. After a delay of D blocks, the transmitter obtains this index and updates the beamforming vector at block $iK + D$.
As shown in Figure 11, the beamforming vector $\mathbf{w}[iK]$ is used from block $iK + D$ to block $iK + D + K - 1$. In block $iK + k$, the $N_r \times 1$ received signal vector can be expressed as

$$\mathbf{y}(iK+k) = \mathbf{H}(iK+k)\mathbf{w}[iK]s(iK+k) + \boldsymbol{\eta}(iK+k)\,,$$

where $s(iK + k) \in \mathbb{C}$ is the data symbol; and $\boldsymbol{\eta}(iK + k)$ denotes the noise vector with i.i.d. $\mathcal{CN}(0, 1)$ entries. The receiver performs maximum ratio combining on the received signal with the combining vector

$$\mathbf{z}(iK+k) = \frac{\mathbf{H}(iK+k)\mathbf{w}[iK]}{\|\mathbf{H}(iK+k)\mathbf{w}[iK]\|^2}\,.$$

Then the post-combining signal is given by

$$\begin{aligned} r(iK+k) &= \mathbf{z}^H(iK+k)\ \mathbf{y}(iK+k) \\ &= s(iK+k) + \frac{\mathbf{w}^*[iK]\mathbf{H}^*(iK+k)}{\|\mathbf{H}(iK+k)\mathbf{w}[iK]\|^2}\,\boldsymbol{\eta}(iK+k). \end{aligned} \tag{79}$$

We assume no temporal power control is used, i.e., the average symbol SNR

$$\gamma_S \triangleq \mathbb{E}\{|s(iK+k)|^2\}/N_0$$

is time-invariant. So the receive SNR of the post-combining signal is given by

$$\gamma(iK+k) = \gamma_S\left\|\mathbf{H}(iK+k)\mathbf{w}[iK]\right\|^2, \quad k = D, \cdots, D+K-1. \tag{80}$$

4.2 SER analysis

We assume PSK signal in the analysis. Conditioned on the instantaneous SNR, the symbol error probability of M-ary PSK is given by Equation (7) shown at the beginning of Section 2.2. Therefore, according to (80), the SER at block $iK + k, k = D, \cdots, D + K - 1$, can be written as

$$\begin{aligned} P_e(iK+k) &= \frac{1}{\pi}\,\mathbb{E}\left\{\int_0^{\frac{(M-1)\pi}{M}} \exp\left(-\frac{g_{\mathrm{PSK}}\gamma(iK+k)}{\sin^2\theta}\right)\mathrm{d}\theta\right\}. \\ &= \frac{1}{\pi}\int_0^{\frac{(M-1)\pi}{M}} \mathbb{E}\,\exp\left(-\frac{g_{\mathrm{PSK}}\gamma_S}{\sin^2\theta}\left\|\mathbf{H}(iK+k)\mathbf{w}[iK]\right\|^2\right)\mathrm{d}\theta\,. \end{aligned} \tag{81}$$

where $g_{\mathrm{PSK}} = \sin^2(\pi/M)$ depends on the constellation size.
According to (77) (78), the beamforming vector $\mathbf{w}[iK]$ is determined by the channel matrices $\mathbf{H}(iK - p), p = 0, \cdots, P$. Then $P_e(iK + k)$ depends on the joint distribution of $\mathbf{H}(iK + k)$ and $\mathbf{H}(iK - p), p = 0, \cdots, P$. Since this joint distribution is related to k and independent of i, so is

$P_e(iK+k)$. That is, $P_e(iK+k)$ is periodic with period K. Therefore we can confine our attention to just one period, and calculate the average SER of the system according to

$$\begin{aligned}\overline{P}_e &= \frac{1}{K}\sum_{k=D}^{D+K-1} P_e(iK+k)\big|_{\,i=0} \\ &= \frac{1}{\pi K}\sum_{k=D}^{D+K-1}\frac{1}{\pi}\int_0^{\frac{(M-1)\pi}{M}} \mathbb{E}\,\exp\left(-\frac{g\gamma_S}{\sin^2\theta}\left\|\mathbf{H}(k)\mathbf{w}[0]\right\|^2\right)\mathrm{d}\theta \end{aligned} \tag{82}$$

Since the random variables $\mathbf{H}(k)$ and $\mathbf{w}[0]$ in (82) are both related to the channel prediction $\widehat{\mathbf{H}}[0]$, some relationship can be established between the expectation in (82) and the statistics of the channel prediction, as shown in the following lemma.

Lemma 5. *Given $t \geq 0$ and $k = D, \cdots, D+K-1$, we have*

$$\mathbb{E}\,\exp\left(-t\left\|\mathbf{H}(k)\mathbf{w}[0]\right\|^2\right) = \left(\frac{1}{1+t\,\beta(k)}\right)^{N_r}\mathbb{E}\,\exp\left(-\frac{t\,[1-\beta(k)]}{1+t\,\beta(k)}\max_{\mathbf{c}\in\mathcal{C}}\left\|\sigma_{\mathrm{Prd}}^{-1}\widehat{\mathbf{H}}[0]\mathbf{c}\right\|^2\right), \tag{83}$$

where the parameters

$$\beta(k) \triangleq 1 - \frac{\left|\sum_{p=0}^{P} a(p)J_0(2\pi f_d T_B|p+k|)\right|^2}{\sum_{p=0}^{P}\sum_{q=0}^{P} a^*(p)a(q)J_0(2\pi f_d T_B|p-q|)}, \tag{84}$$

$$\sigma_{\mathrm{Prd}} \triangleq \sqrt{\sum_{p=0}^{P}\sum_{q=0}^{P} a^*(p)a(q)J_0(2\pi f_d T_B|p-q|)}, \tag{85}$$

depends on the predictor coefficients $a(0), \cdots, a(P)$.

Proof: By the law of total expectation, the left-hand-side of (83) can be written as

$$\mathbb{E}\exp\left(-t\left\|\mathbf{H}(k)\mathbf{w}[0]\right\|^2\right) = \mathbb{E}\Big\{\mathbb{E}\Big[\exp\left(-t\left\|\mathbf{H}(k)\mathbf{w}[0]\right\|^2\right)\Big|\widehat{\mathbf{H}}[0]\Big]\Big\}. \tag{86}$$

The inner expectation in the right-hand-side of (25) depends on the conditional distribution of $\left(\mathbf{H}(k)\big|\widehat{\mathbf{H}}[0]\right)$, which can be obtained as follows. For the (m,n)th channel branch, the channel prediction is given by $\hat{h}_{m,n}[0] = \sum_p a^*(p)h_{m,n}(-p)$. Since the channel coefficients are jointly Gaussian, the conditional distribution of $\left(h_{m,n}(k)|\hat{h}_{m,n}[0]\right)$ must be Gaussian. This type of conditional distribution has been well studied in the literature. Applying the existing result to our case, we can easily obtain the conditional mean and variance, and write

$$\left(\,h_{m,n}(k)\,|\,\hat{h}_{m,n}[0]\,\right) \sim \mathcal{CN}\left(\,\rho(k)\hat{h}_{m,n}[0]\,,\,\beta(k)\right), \quad m = 1,\cdots,N_r,\ n = 1,\cdots,N_t, \tag{87}$$

where $\beta(k)$ is given by (84) and

$$\rho(k) \triangleq \frac{\sum_{p=0}^{P} a(p)J_0(2\pi f_d T_B|p+k|)}{\sum_{p=0}^{P}\sum_{q=0}^{P} a^*(p)a(q)J_0(2\pi f_d T_B|p-q|)}. \tag{88}$$

Since no spatial correlation exists, the result of (87) implies that $\left(\mathbf{H}(k)\big|\widehat{\mathbf{H}}[0]\right)$ is matrix-Gaussian distributed with mean $\rho(k)\widehat{\mathbf{H}}[0]$ and covariance $\beta(k)\,\mathbf{I}_{N_r}\otimes\mathbf{I}_{N_t}$. To proceed,

notice that $\mathbf{w}[0]$ is a *unit-norm* codeword determined by $\widehat{\mathbf{H}}[0]$. Then conditioned on $\widehat{\mathbf{H}}[0]$, $\mathbf{H}(k)\mathbf{w}[0]$ is a Gaussian random vector with mean $\rho(k)\widehat{\mathbf{H}}[0]\mathbf{w}[0]$ and covariance $\beta(k)\,\mathbf{I}_{N_r}$. So the inner expectation in the right-hand-side of (86) can be derived as [Zhou & Giannakis (2004), Eq.(36)]

$$\mathbb{E}\Big[\exp\left(-t\,\|\mathbf{H}(k)\mathbf{w}[0]\|^2\right)\Big|\,\widehat{\mathbf{H}}[0]\Big] = \left(\frac{1}{1+t\,\beta(k)}\right)^{N_r}\exp\left(-\frac{t\,\rho^2(k)\big\|\widehat{\mathbf{H}}[0]\mathbf{w}[0]\big\|^2}{1+t\,\beta(k)}\right). \tag{89}$$

Substituting (89) into (86) and noticing

$$\big\|\widehat{\mathbf{H}}[0]\mathbf{w}[0]\big\|^2 = \max_{\mathbf{c}\in\mathcal{C}}\big\|\widehat{\mathbf{H}}[0]\mathbf{c}\big\|^2, \qquad \rho^2(k) = \sigma_{\text{Prd}}^{-2}\left[1-\beta(k)\right],$$

we reach the desired result of (83). □

Applying (83) to (82), the average SER can be written as

$$\begin{aligned}\overline{P}_e = \frac{1}{\pi K}\sum_{k=D}^{D+K-1}\int_0^{\frac{(M-1)\pi}{M}}&\left(\frac{\sin^2\theta}{\sin^2\theta+g_{\text{PSK}}\gamma_S\beta(k)}\right)^{N_r}\\ &\times\mathbb{E}\exp\left(-\frac{g_{\text{PSK}}\gamma_S[1-\beta(k)]}{\sin^2\theta+g_{\text{PSK}}\gamma_S\beta(k)}\max_{\mathbf{c}\in\mathcal{C}}\big\|\sigma_{\text{Prd}}^{-1}\widehat{\mathbf{H}}[0]\mathbf{c}\big\|^2\right)\,\mathrm{d}\theta\,.\end{aligned} \tag{90}$$

In (90), we treat $\sigma_{\text{Prd}}^{-1}\widehat{\mathbf{H}}[0]$ as a random matrix, whose distribution can be obtained as follows. The entries of $\widehat{\mathbf{H}}[0]$ must be Gaussian and independent of each other, because the predictor is linear and the channel is spatially white. Using (76) (77), it is can be verified that all entries of $\widehat{\mathbf{H}}[0]$ have zero mean and variance σ_{Prd}^2. This implies that $\sigma_{\text{Prd}}^{-1}\widehat{\mathbf{H}}[0]$ is an $N_r\times N_t$ random matrix with i.i.d. $\mathcal{CN}(0,1)$ entries. Therefore Lemma 1 in Section 2.2 can be applied to the right-hand-side of (90). After some manipulations, we obtain the following upper bound on the average SER

$$\overline{P}_e \le \frac{1}{\pi K}\sum_{k=D}^{D+K-1}\int_0^{\frac{(M-1)\pi}{M}}\frac{\sin^{2N_r}\theta\left[\sin^2\theta+g_{\text{PSK}}\gamma_S\beta(k)\right]^{(N_t-1)N_r}}{\left[\sin^2\theta+g_{\text{PSK}}\gamma_S\beta(k)+g_{\text{PSK}}g_{\text{CB}}\gamma_S(1-\beta(k))\right]^{N_tN_r}}\,\mathrm{d}\theta\,, \tag{91}$$

which is the main result of the SER analysis. Note that the value of the codebook-dependent parameter g_{CB} can be calculated numerically according to (11), or using the closed-form approximation (15).

4.3 Predictor design

We will utilize the SER bound (91) to a design good predictor in terms of error performance. But the integral in the bound complicates the optimization problem. To make the problem tractable, we focus on high SNR regime. When γ_S is large, the "$\sin^2\theta$" in the denominator of (91) can be omitted. and the following inequality is obtained

$$\begin{aligned}&\frac{\sin^{2N_r}\theta\left[g_{\text{PSK}}\gamma_S\beta(k)\right]^{(N_t-1)N_r}}{\left[g_{\text{PSK}}\gamma_S\beta(k)+g_{\text{PSK}}g_{\text{CB}}\gamma_S(1-\beta(k))\right]^{N_tN_r}}\\ \ge\ &\frac{\sin^{2N_r}\theta\left[\sin^2\theta+g_{\text{PSK}}\gamma_S\beta(k)\right]^{(N_t-1)N_r}}{\left[\sin^2\theta+g_{\text{PSK}}\gamma_S\beta(k)+g_{\text{PSK}}g_{\text{CB}}\gamma_S(1-\beta(k))\right]^{N_tN_r}}\end{aligned}$$

Therefore, the average SER can be further upper bounded by

$$\overline{P}_e \leq \frac{1}{\pi K (g_{\mathrm{PSK}}\gamma_S)^{N_r}} \left[\int_0^{\frac{(M-1)\pi}{M}} \sin^{2N_r}\theta \, \mathrm{d}\theta \right] \sum_{k=D}^{D+K-1} \frac{[\beta(k)]^{(N_t-1)N_r}}{\left[\beta(k) + g_{\mathrm{CB}}(1-\beta(k))\right]^{N_t N_r}} . \tag{92}$$

It is observed that the SER decreases at a speed of $\gamma_S^{-N_r}$, i.e., the diversity order is N_r. Since full diversity order $N_t N_r$ can be achieved by finite-rate beamforming without feedback delay [Love & Heath (2005)], the diversity from transmit antennas is lost due to feedback delay.
Based on (92), the predictor design can be formulated as a minimization problem. To get a concise description, we collect the predictor coefficients into a vector $\mathbf{a} \triangleq [a(0), \cdots, a(P)]^T$, and define the following notations

- The temporal correlation matrix $\mathbf{R} \in \mathbb{C}^{(P+1)\times(P+1)}$, with the (p,q)-th entry

$$[\mathbf{R}]_{p,q} \triangleq J_0(2\pi f_d T_B |p-q|), \quad p,q = 0,1,\cdots,P. \tag{93}$$

- The cross-correlation vector $\mathbf{r}(k) \in \mathbb{C}^{(P+1)}$ with lag k, $k = D, \cdots, D+K-1$. The p-th entry of $\mathbf{r}(k)$ is

$$[\mathbf{r}(k)]_p \triangleq J_0(2\pi f_d T_B |p+k|), \quad p = 0,1,\cdots,P. \tag{94}$$

In the right-hand-side of (92), only the parameter $\beta(k)$ is related to the predictor. So only the summation needs to be considered in the predictor design. Since

$$\beta(k) = 1 - |\mathbf{r}^*(k)\,\mathbf{a}|^2 / \mathbf{a}^*\mathbf{R}\mathbf{a}$$

by definition, the summation in (92) can be expressed as

$$\sum_{k=D}^{D+K-1} \frac{\left[\mathbf{a}^*\mathbf{R}\mathbf{a}\right]^{N_r} \left[\mathbf{a}^*\mathbf{R}\mathbf{a} - |\mathbf{r}^*(k)\,\mathbf{a}|^2\right]^{(N_t-1)N_r}}{\left[\mathbf{a}^*\mathbf{R}\mathbf{a} - (1-g_{\mathrm{CB}})\,|\mathbf{r}^*(k)\,\mathbf{a}|^2\right]^{N_t N_r}} , \tag{95}$$

which is used as the metric of the predictor design. Because a coefficient vector $\mathbf{a}$ and its "normalized" version $\mathbf{a}/\sqrt{\mathbf{a}^*\mathbf{R}\mathbf{a}} \in \{\mathbf{x} : \mathbf{x}^*\mathbf{R}\mathbf{x} = 1\}$ yield the same value of (95), we impose the constraint $\mathbf{a}^*\mathbf{R}\mathbf{a} = 1$, and propose the following predictor design criterion

$$\begin{aligned} \underset{\mathbf{a}}{\text{minimize}} \; : \; & \sum_{k=D}^{D+K-1} \frac{\left[1 - |\mathbf{r}^*(k)\,\mathbf{a}|^2\right]^{(N_t-1)N_r}}{\left[1-(1-g_{\mathrm{CB}})\,|\mathbf{r}^*(k)\mathbf{a}|^2\right]^{N_t N_r}} \\ \text{subject to} \; : \; & \mathbf{a}^*\mathbf{R}\mathbf{a} = 1 . \end{aligned} \tag{96}$$

The closed-form solution to (96) is hard to obtain. So we have to use numerical methods to solve it. Since the predictor can be designed offline, the computational complexity is affordable. However, there are still some issues that need to be addressed.

a) The minimization problem (96) is not always convex. (The convexity of the cost function depends on the values of $N_t, N_r, g_{\mathrm{CB}}$.) For a non-convex problem, most optimization algorithms can only guarantee convergence to a local minimum, i.e., a suboptimal solution.

b) An initial value for numerical methods can be obtained in a heuristic way. In the summation in (96), the term with index $k = D$ is a decreasing function of $|\mathbf{r}^*(D)\,\mathbf{a}|^2$. The predictor that maximizes $|\mathbf{r}^*(k)\,\mathbf{a}|^2$ under the constraint $\mathbf{a}^*\mathbf{R}\mathbf{a} = 1$ is given by

$$\mathbf{a}_{\mathrm{ini}} = \left[\mathbf{r}^*(D)\mathbf{R}^{-1}\mathbf{r}(D)\right]^{-\frac{1}{2}} \mathbf{R}^{-1}\mathbf{r}(D) . \tag{97}$$

This initial value gives satisfactory results in our simulations.

	3Tx-2Rx system	2Tx-2Rx system
Antenna Configuration	$N_t = 3, N_r = 2$	$N_t = N_r = 2$
Codebook	3 bit ($N_c = 8$)	2 bit ($N_c = 4$)
Channel correlation	Jakes' model	
Carrier frequency	1.8 GHz	
Block period (T_B)	1/3 ms	
Terminal speed	60 km/h	30 — 120 km/h
Doppler spread (f_d)	100 Hz	50 — 200 Hz
Feedback interval (K)	6 blocks	4 blocks
Feedback delay (D)	6 blocks	2, 4, 6 blocks
Predictor order (P)	2, 8, 16, 86	8
Modulation	QPSK	
Average symbol SNR	0 — 30 dB	15 dB

Table 2. System parameters in numerical simulations.

c) The temporal correlation matrix $\mathbf{R}$ (defined in (93)) is ill-conditioned (see [Baddour & Beaulieu (2005), Section III-B] and references therein). To avoid possible numerical instability, one may add a small perturbation, namely, replacing $\mathbf{R}$ by $\mathbf{R} + \epsilon\mathbf{I}$, where ϵ is a small positive number.

4.4 Numerical results

Numerical results are presented for a 3Tx-2Rx system and a 2Tx-2Rx system, as specified in Table 2. In both systems, the average feedback rate B/KT_B is fixed at 1.5 kbps. This feedback rate is adopted in 3GPP specifications. Moreover, we use the beamforming codebooks listed in [Love & Heath (2003)].

Predictors are designed by solving (96). Specifically, we use the `fmincon` function in MATLAB and the initial value given in (97). To avoid possible numerical instability, the correlation matrix $\mathbf{R}$ is replaced by $\mathbf{R} + (1.6 \times 10^{-3})\mathbf{I}$. We also consider the case of *delayed feedback* [Huang et al. (2006); Ma & Zhang (2007); Ma et al. (2008)]. This case is equivalent to a trivial zeroth order channel predictor with a single coefficient $a(0) = 1$. The results in Section 4.2 and 4.3 are applicable to this case (setting $P = 0$ and $a(0) = 1$).

Figure 12 illustrates the SER of the 3Tx-2Rx system for different symbol SNR's and predictor orders. We can see that compared with delayed feedback, even the 2nd order predictor improves the error performance considerably. The SER decreases with the increase of the predictor order, but the decrease of SER is no longer remarkable when $P > 16$. It is also observed that the analytical result (91) is tight, and the diversity gain is 2, as discussed in Section IV-A.

Figure 13 depicts the SER of the 2Tx-2Rx system for different terminal speeds and feedback delays. It is shown that the system with channel prediction is more robust to the movement of the terminal. However, the SER is sensitive to the value of the feedback delay D both in the case of delayed feedback and in the case of predicted feedback.

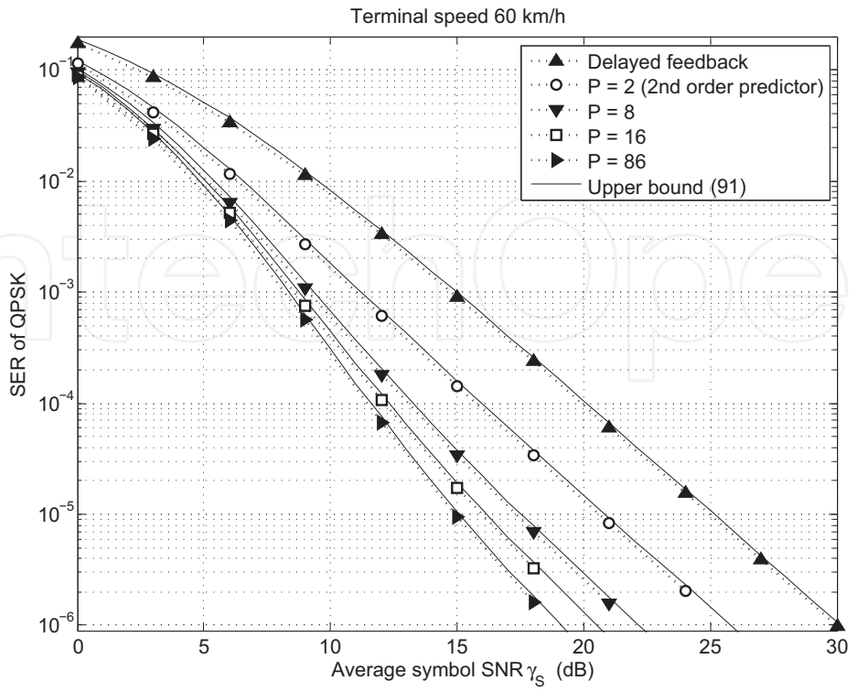

Fig. 12. SER performance of the 3Tx-2Rx system.

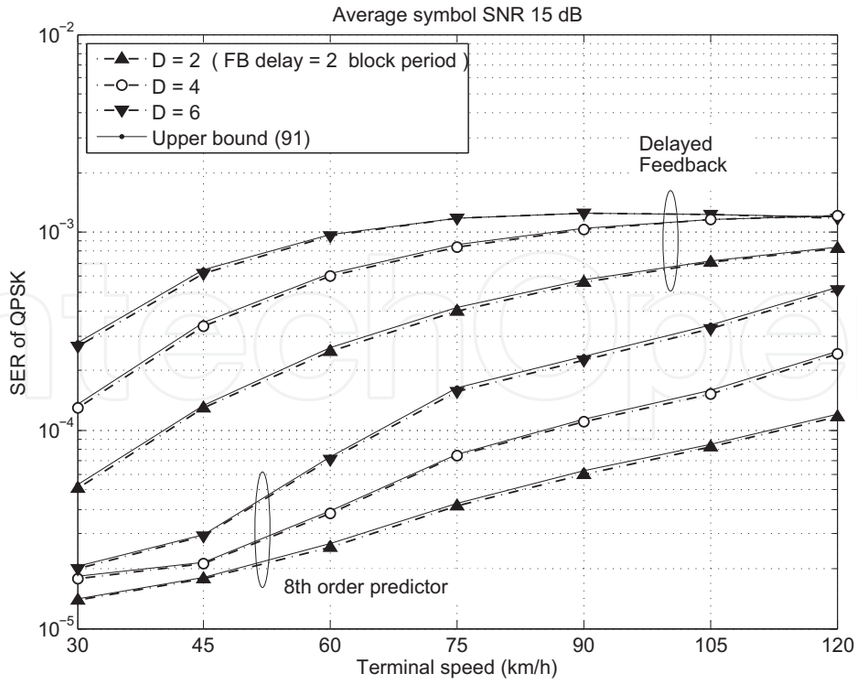

Fig. 13. SER performance of the 2Tx-2Rx system.

5. Conclusion

This chapter highlighted recent advances in beamforming based on finite-rate feedback from a communication-theoretic perspective. We first studied the SER performance of the finite-rate beamforming system. In a Rayleigh fading environment, an upper bound on the average SER was derived, which has a simple structure and is tight at all SNRs. Secondly, feedback error problem in a finite-rate beamforming system was investigated. The effect of feedback error on the diversity and array gains was quantified analytically. Index assignment technique was introduced to provide a redundancy-free protection against feedback error, and a good index assignment scheme was designed to maximize the array gain. Thirdly, we investigated the effect of feedback delay on finite-rate beamforming, and proposed to use a channel prediction scheme to compensate the performance degradation. For a beamforming system with delayed finite-rate feedback, an upper bound on the SER was derived, and a predictor was designed to provide good SER performance. The derived analytical results and the proposed performance enhancement schemes in this section were all verified by simulations under typical system configurations.

6. References

P. A. Dighe, R. K. Mallik, and S. S. Jamuar, "Analysis of transmit-receive diversity in Rayleigh fading," *IEEE Trans. Commun.*, vol. 51, no. 4, pp. 694-703, Apr. 2003.

P. A. Dighe, R. K. Mallik, and S. S. Jamuar, "Analysis of *K*-transmit dual-receive diversity with cochannel interferers over a Rayleigh fading channel," *Wireless Personal Communications*, vol. 25, no. 2, pp. 87-100, 2003.

Q. Zhou and H. Dai, "Asymptotic analysis in MIMO MRT/MRC systems," *EURASIP J. Wireless Commun. Net.*, 2006.

M. Kang, and M.-S. Alouini, "A comparative study on the performance of MIMO MRC systems with and without cochannel interference," *IEEE Trans. Commun.*, vol.52, no.8, pp.1417-1425, Aug. 2004.

K. K. Mukkavilli, A. Sabharwal, B. Aazhang, and E. Erkip, "On beamforming with finite rate feedback in multiple-antenna systems," *IEEE Trans. Inform. Theory*, vol. 49, no. 10, pp. 2562-2579, Oct. 2003.

D. J. Love, and R. W. Heath, Jr., "Grassmannian beamforming for multiple-input multiple-output wireless systems," *IEEE Trans. Inform. Theory*, vol. 49, no. 10, pp. 2735-2747, Oct. 2003.

D. J. Love, and R. W. Heath, Jr., "Necessary and sufficient conditions for full diversity order in correlated Rayleigh fading beamforming and combining systems," *IEEE Trans. Wireless Commun.*, vol. 4, pp. 20-23, Jan. 2005.

P. Xia, and G. B. Giannakis, "Design and analysis of transmit-beamforming based on limited-rate feedback," *IEEE Trans. Signal Process.*, vol. 54, pp. 1853-1862, May 2006.

S. Zhou, and G. B. Giannakis, "How accurate channel prediction needs to be for transmit-beamforming with adaptive modulation over Rayleigh MIMO channels?" *IEEE Trans. Wireless Commun.*, vol. 3, no. 4, pp. 1285-1294, July 2004.

S. Zhou, Z. Wang, and G. B. Giannakis, "Quantifying the power loss when transmit beamforming relies on finite-rate feedback," *IEEE Trans. Wireless Commun.*, vol. 4, pp. 1948-1957, July. 2005.

B. Mondal, and R. W. Heath, Jr., "Performance analysis of quantized beamforming MIMO systems," *IEEE Trans. Signal Process.*, vol. 54, no. 12, pp. 4753-4766, Dec. 2006.

K. Huang, B. Mondal, R. W. Heath, Jr., and J. G. Andrews, "Effect of feedback delay on multi-antenna limited feedback for temporally-correlated channels," in *Proc. Globecom*, San Francisco, CA, Nov.27-Dec.1, 2006.

Y. Ma, and D. Zhang, "Error Rate of Transmit Beamforming with Delayed and Limited Feedback," in *Proc. Globecom*, Washington, DC, Nov. 26-30, 2007.

Y. Ma, A. Leith, and R. Schober, "Predictive feedback for transmit beamforming with delayed feedback and channel estimation errors," in *Proc. ICC*, Beijing, China, May 19-23, 2008.

K. Zeger, and A. Gersho, "Pseudo-Gray coding," *IEEE Trans. Commun.*, vol.38, no.12, pp.2147-2158, Dec. 1990.

G. Ben-David, and D. Malah, "Bounds on the performance of vector-quantizers under channel errors," *IEEE Trans. Inform. Theory*, vol.51, no.6, pp.2227-2235, June 2005.

T. L. Marzetta, and B. M. Hochwald, "Capacity of a mobile multiple-antenna communication link in Rayleigh flat fading," *IEEE Trans. Inform. Theory*, vol.45, no.1, pp.139-157, Jan. 1999.

K. E. Baddour, and N. C. Beaulieu, "Autoregressive Modeling for Fading Channel Simulation," *IEEE Trans. Wireless Commun.*, vol. 4, no. 4, pp. 1650-1662, July 2005.

P. Zhu, L. Tang, Y. Wang, and X. You, "Index Assignment for Quantized Beamforming MIMO Systems," *IEEE Trans. Wireless Commun.*, vol. 7, no. 8, pp. 2917 - 2922, Aug. 2008.

P. Zhu, L. Tang, Y. Wang, and X. You, "Quantized beamforming with channel prediction," *IEEE Trans. Wireless Commun.*, vol. 8, no. 11, pp. 5377 - 5382, Nov. 2009.

P. Zhu, L. Tang, Y. Wang, and X. You, "An upper bound on the SER of transmit beamforming in correlated Rayleigh fading," *IEEE Trans. Commun.*, vol. 58, no. 2, pp. 457 - 462, Feb. 2010.

M. K. Simon, and M. -S. Alouini, *Digital communication over fading channels*, 2nd Ed., Wiley, 2005.

D. Tse, and P. Viswanath, *Fundamentals of wireless communication*, Cambridege University Press, 2005.

W. Fleming, *Functions of several variables*, 2nd Ed., Spinger-Verlag, 1977.

D. J. Love. (2006, Nov.) Personal Webpage on Grassmannian Subspace Packing. [Online]. Available: http://cobweb.ecn.purdue.edu/~djlove/ grass.html

Third Generation Partnership Project (3GPP), "Physical channels and modulation," 3GPP TS 36.211 V8.2.0, Mar. 2008.

V. Erceg, *et al.*, "TGn channel models," IEEE 802.11-03/940r4, May 2004.

MIMO Systems, Theory and Applications

Edited by Dr. Hossein Khaleghi Bizaki

ISBN 978-953-307-245-6
Hard cover, 488 pages
Publisher InTech
Published online 04, April, 2011
Published in print edition April, 2011

In recent years, it was realized that the MIMO communication systems seems to be inevitable in accelerated evolution of high data rates applications due to their potential to dramatically increase the spectral efficiency and simultaneously sending individual information to the corresponding users in wireless systems. This book, intends to provide highlights of the current research topics in the field of MIMO system, to offer a snapshot of the recent advances and major issues faced today by the researchers in the MIMO related areas. The book is written by specialists working in universities and research centers all over the world to cover the fundamental principles and main advanced topics on high data rates wireless communications systems over MIMO channels. Moreover, the book has the advantage of providing a collection of applications that are completely independent and self-contained; thus, the interested reader can choose any chapter and skip to another without losing continuity.

InTech Europe
University Campus STeP Ri
Slavka Krautzeka 83/A
51000 Rijeka, Croatia
Phone: +385 (51) 770 447
Fax: +385 (51) 686 166
www.intechopen.com

InTech China
Unit 405, Office Block, Hotel Equatorial Shanghai
No.65, Yan An Road (West), Shanghai, 200040, China
中国上海市延安西路65号上海国际贵都大饭店办公楼405单元
Phone: +86-21-62489820
Fax: +86-21-62489821

IntechOpen